

## Probe Report

**Title:** Optimization and characterization of a triazole urea inhibitor for alpha/beta hydrolase domain-containing protein 11 (ABHD11): anti-probe for LYPLA1/LYPLA2 dual inhibitor ML211

**Authors:** Alexander Adibekian\*, Ku-Lung Hsu\*, Anna E Speers\*, Steven J Brown\*, Timothy Spicer<sup>†</sup>, Virneliz Fernandez-Vega<sup>†</sup>, Jill Ferguson\*, Benjamin F Cravatt\*, Peter Hodder<sup>†</sup>, and Hugh Rosen\*

\*The Scripps Research Institute, La Jolla CA; <sup>†</sup>The Scripps Research Institute, Jupiter, FL  
Corresponding author: [hrosen@scripps.edu](mailto:hrosen@scripps.edu)

**Assigned Assay Grant #:** 1 R01 CA132630

**Screening Center Name & PI:** The Scripps Research Institute Molecular Screening Center (SRIMSC), H Rosen

**Chemistry Center Name & PI:** SRIMSC, H Rosen

**Assay Submitter & Institution:** BF Cravatt, TSRI, La Jolla

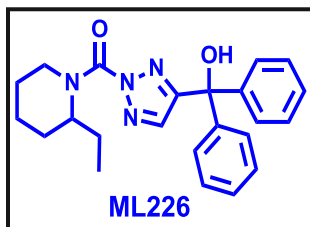
**PubChem Summary Bioassay Identifier (AID):** 2202 (LYPLA1), 2203 (LYPLA2)

## Abstract

Protein palmitoylation is an essential post-translational modification necessary for trafficking and localization of regulatory proteins that play key roles in cell growth and signaling. Multiple oncogenes, including HRAS and SRC, require palmitoylation for malignant transformation. We [1] and others [2] have previously identified lysophospholipase 1 (LYPLA1) as a candidate protein palmitoyl thioesterase responsible for HRAS depalmitoylation in mammalian cells. Seeking chemical tools to investigate biochemical pathway involvement and potential roles in cancer pathogenesis, we conducted a fluorescence polarization-based competitive activity-based protein profiling (FluoPol ABPP) [3] high throughput screening (HTS) campaign to identify inhibitors of LYPLA1 and the structurally related LYPLA2. HTS identified a micromolar triazole urea inhibitor, that we successfully optimized via several rounds of SAR-by-synthesis as **ML211** (SID 99445338), a low nanomolar dual inhibitor of LYPLA1 and LYPLA2. The reported probe operates by a covalent mechanism of action and is active both *in vitro* and *in situ*. Out of more than 20 serine hydrolases (SHs) profiled by gel-based competitive activity-based protein profiling (ABPP), **ML211** was observed to have one anti-target, alpha/beta hydrolase domain-containing protein 11 (ABHD11). Fortuitously, one of the triazole urea library members synthesized during the course of probe optimization was found to be a potent and selective inhibitor of ABHD11, a poorly characterized SH that is hemizygotously deleted in Williams-Beuren syndrome [4], and was presented as a control anti-probe (SID 99445332) in the **ML211** Probe Report. The optimized ABHD11 probe **ML226** is a potent inhibitor of ABHD11, with an IC<sub>50</sub> of 15 nM, and exhibits at least 100-fold selectivity for all other SHs (~20) assessed by gel-based competitive ABPP. The probe is also active *in situ*, completely and selectively inhibiting

ABHD11 at sub-nanomolar concentrations. As with **ML211**, the probe operates by a covalent mechanism of action, carbamoylating the active site serine of ABHD11. The complete properties, characterization, and synthesis of **ML226** are detailed in this Probe Report.

### Probe Structure & Characteristics



CID/ML#	Target Name	Target IC50 (nM) [SID, AID]	Anti-target Name(s)	Anti-target IC50 (nM) [SID, AID]	Fold Selective <sup>†</sup>	Secondary Assay(s) Name: IC50 (nM) [SID, AID]
CID 56593112/ <b>ML226</b>	ABHD11	15 [SID 99445332, AID 504507]	>20 SHs*	≥1500 [SID 99445332, AID 493111]**	≥100	<b>Inhibition Assay:</b> [SID 99445332, AIDs 493111 and 504520] <b>Selectivity Assay:</b> [SID 99445332, AIDs 493111 and 504520] <b>SILAC Selectivity Assay:</b> [SID 99445332, AID 504522] <b>In Situ Assay:</b> [SID 99445332, AID 504505] <b>IC50 Assay (in vitro):</b> 15 nM [SID 99445332, AID 504507] <b>IC50 Assay (in situ):</b> 0.68 nM [SID 99445332, AID 504482] <b>Cytox assay:</b> [SID 99445332, AID 504510] <b>LC-MS/MS assay:</b> [SID 99445332, AID 504498]
<p>* As assessed by gel-based competitive ABPP in a soluble proteome derived from murine T cells with the serine hydrolase probe FP-Rhodamine</p> <p>** IC50 of the anti-target is defined as greater than the test compound concentration at which less than or equal to 50% inhibition of the anti-target is observed, which is reported in AID 493111. For SID 99445332, of all serine hydrolases (SHs) assayed, only APEH showed 50% INH at 1500 nM concentration, so the IC50 is reported as ≥ 1500 nM.</p> <p>† Fold-selectivity was calculated as: ≥IC50 for anti-target/IC50 for target</p>						

### Recommendations for Scientific Use of the Probe

Protein palmitoylation is an essential post-translational modification (PTM), and identification of enzymes responsible for the dynamic modulation of palmitoylation is paramount to understanding its patho/physiological roles. We [1] and others [2] have previously identified LYPLA1 as a putative protein palmitoyl thioesterase capable of regulating HRAS palmitoylation in mammalian cells. LYPLA2 is 65% identical to LYPLA1, but its potential role as a thioesterase is unknown. We previously reported a dual LYPLA1/LYPLA2 inhibitor, **ML211**, that is active both *in vitro* (complex proteome lysates) and *in situ* (cells in culture) at low nanomolar concentration. The probe was observed to have one anti-target, the serine hydrolase (SH) ABHD11. The

specific



ABHD11 inhibitor, **ML226**, described herein, is to be used as a control for identification of ABHD11-selective phenotypes in primary research studies aimed at elucidating the patho/physiological roles of LYPLA1 and LYPLA2, as well as investigating the biology of ABHD11 and its potential role in Williams-Beuren syndrome.

## 1 Introduction

Protein palmitoylation is an essential post-translational modification necessary for trafficking and localization of regulatory proteins that play key roles in cell growth and signaling, and identification of proteins responsible for the dynamic modulation of palmitoylation is paramount to understanding its patho/physiological roles. For example, it has been suggested by Waldmann et al. that preventing depalmitoylation of the oncogene Ras by inhibiting thioesterase activity may disrupt targeted distribution, thereby downregulating oncogenic signaling [2]. As such, inhibitors of protein palmitoyl thioesterases may act as tumor suppressors by preventing aberrant growth signaling. More than a decade ago, the cytosolic serine hydrolase (SH) acyl-protein thioesterase 1 (APT1) was identified as an *in vitro* HRAS palmitoyl thioesterase [5]. Initially classified as lysophospholipase 1 (LYPLA1) [6], the enzyme has since been demonstrated to have several hundred-fold higher activity as a protein thioesterase. Upon retroviral shRNA knockdown of LYPLA1, we found that over-expressed HRAS was hyper-palmitoylated, providing evidence that endogenous LYPLA1 a functional protein palmitoyl thioesterase in mammalian cells. LYPLA2 (a.k.a. APT2) is a close homologue of LYPLA1 (65% identical) and exhibits lysophospholipase activity *in vitro*, but its potential role as a thioesterase is unknown [7]. Several inhibitors of LYPLA1 have been described [2, 8-9], but none of these agents have proven capable of selectively inhibiting LYPLA1 activity in cells. No selective inhibitors of LYPLA2 have been reported.

As SHs, the LYPLAs are readily labeled by activity-based protein profiling (ABPP) probes bearing a fluorophosphonate (FP) reactive group [10], which can be exploited for inhibitor discovery using a competitive-ABPP platform, whereby small molecule enzyme inhibition is assessed by the ability to out-compete ABPP probe labeling [11]. Competitive ABPP has also been configured to operate in a high-throughput manner via fluorescence polarization readout, FluoPol-ABPP [3]. Seeking selective, *in situ* active chemical tools to investigate the potential roles of the LYPLAs in cancer pathogenesis, we conducted a FluoPol-ABPP HTS campaign to identify inhibitors of LYPLA1 (AIDs 2174 and 2233) and the structurally related LYPLA2 (AIDs 2177 and 2232). HTS identified a modestly potent triazole urea inhibitor (SID 7974398; IC<sub>50</sub> 795 nM vs. LYPLA1, 5200 nM vs. LYPLA2), which was successfully optimized via several rounds of SAR-by-synthesis as **ML211** (SID 99445338), a low nanomolar dual inhibitor of LYPLA1 (IC<sub>50</sub> 17 nM) and LYPLA2 (IC<sub>50</sub> 30 nM). The triazole urea scaffold has also been developed into inhibitors of other SHs (e.g, see Probe Reports for **ML225**, **ML294**, and **ML295** and ref. [12]. Out of more than 20 SHs profiled by gel-based competitive ABPP, **ML211** is 50-

fold selective for all except for one anti-target, alpha/beta hydrolase domain-containing protein 11 (ABHD11; IC<sub>50</sub> 10 nM). However, during our SAR campaign we fortuitously discovered a selective ABHD11 inhibitor from among the synthetic triazole urea library compounds. This compound **ML226** was presented as an anti-probe in the **ML211** Probe Report for use as a control.

ABHD11 is a poorly characterized SH; all that is known about its biology is that it is a mitochondrial enzyme [13] with broad tissue distribution, has little sequence homology to other proteins, and its gene is located in a region of chromosome 7 that is hemizygotously deleted in Williams-Beuren syndrome, a rare genetic disease with symptoms that include vascular stenosis, mental retardation, and excessive sociability [4]. However, the underlying biology and contribution of ABHD11 to the disease is unknown, as its biochemical function, substrates, and products have not been identified. A principle goal of post-genomic research is the determination of the molecular and cellular roles of uncharacterized enzymes like ABHD11. As such, potent and selective inhibitors of ABHD11 not only serve as key controls for **ML211**, but important chemical tools in their own right for investigation of ABHD11 biology. This Probe Report provides details of the optimization and characterization of the triazole urea probe **ML226**, a potent (IC<sub>50</sub> 15 nM) and selective (100-fold among FP-sensitive SHs) covalent inhibitor that is active against ABHD11 *in vitro* and *in situ*. **ML226** is only the second known selective inhibitor of ABHD11, and is 11-fold more potent than a carbamate-based inhibitor we recently reported [14] (see **section 4.1**).

## 2 Materials and Methods

All reagents for chemical synthesis were obtained from ThermoFisher or SigmaAldrich. All other protocols are summarized in section 2.1.

### 2.1 Assays

#### Probe Characterization Assays

##### Solubility

The solubility of compounds was tested in phosphate buffered saline, pH 7.4. Compounds were inverted for 24 hours in test tubes containing 1-2 mg of compound with 1 mL of PBS. The samples were centrifuged and analyzed by HPLC (Agilent 1100 with diode-array detector). Peak area was compared to a standard of known concentration.

##### Stability

Demonstration of stability in PBS was conducted under conditions likely to be experienced in a laboratory setting. The compound was dissolved in 1 mL of PBS at a concentration of 10 µM, unless its maximum solubility was insufficient to achieve this concentration. Low solubility

compounds were tested between ten and fifty percent of their solubility limit. The solution was immediately aliquoted into seven standard polypropylene microcentrifuge tubes which were stored at ambient temperature in a block microcentrifuge tube holder. Individual tubes were frozen at -80°C at 0, 1, 2, 4, 8, 24, and 48 hours. The frozen samples were thawed in at room temperature and an equal volume of acetonitrile was added prior to determination of concentration by LC-MS/MS.

### **LC-MS/MS for stability assay**

All analytical methods are in MRM mode where the parent ion is selected in Q1 of the mass spectrometer. The parent ion is fragmented and a characteristic fragment ion is monitored in Q3. MRM mass spectroscopy methods are particularly sensitive because additional time is spent monitoring the desired ions and not sweeping a large mass range. Method development is set up rapidly using Automaton<sup>®</sup> (Applied Biosystems), where the compounds are listed with their name and mass in an Excel datasheet. Compounds are submitted in a 96-well plate to the HPLC autosampler and are slowly injected without a column present. A narrow range centered on the indicated mass is scanned to detect the parent ion. The software then evaluates a few pre-selected parameters to determine conditions that maximize the signal for the parent ion. The molecule is then fragmented in the collision cell of the mass spectrometer and fragments with m/z larger than 70 but smaller than the parent mass are determined. Three separate collision energies are evaluated to fragment the parent ion and the largest three ions are selected. Each of these three fragment ions is further optimized and the best fragment is chosen. The software then inserts the optimized masses and parameters into a template method and saves it with a unique name that indicates the individual compound being optimized. Spectra for the parent ion and the fragmentation pattern are saved and can be reviewed later.

### **Determination of glutathione reactivity**

One µL of a 10 mM compound stock solution was added to 1 mL of a freshly prepared solution of 100 µM reduced glutathione. Final compound concentration is 10 µM unless solubility limited. The solution was allowed to incubate at 37°C for two hours prior to being directly analyzed for glutathione adduct formation. LC-MS/MS analysis of GSH adducts was performed on an API 4000 Q-Trap<sup>TM</sup> mass spectrometer equipped with a Turboionspray source (Applied Biosystems, Foster City, CA). Two methodologies were utilized—a negative precursor ion (PI) scan of m/z 272, corresponding to GSH fragmenting at the thioether bond, and a neutral loss scan of -129 AMU to detect GSH adducts. This triggered positive ion enhanced resolution and enhanced product ion scans [15-16].

### **Primary Assays**

#### **Primary uHTS assay to identify LYPLA1 inhibitors (AID 2174)**

**Assay Overview:** The purpose of this assay was to identify compounds that act as LYPLA1 inhibitors. This assay also serves as a counterscreen for a set of previous experiments entitled, "Fluorescence polarization-based primary biochemical high throughput screening assay to

identify inhibitors of Protein Phosphatase Methyltransferase 1 (PME-1)" (AID 2130). This competitive activity-based protein profiling (ABPP) assay uses fluorescence polarization to investigate enzyme-substrate functional interactions based on active site-directed molecular probes. A fluorophosphonate-rhodamine (FP-Rh) probe, which broadly targets enzymes from the SH family was used to label LYPLA1 in the presence of test compounds. The reaction was excited with linear polarized light and the intensity of the emitted light was measured as the polarization value (mP). As designed, test compounds that act as LYPLA1 inhibitors will prevent LYPLA1-probe interactions, thereby increasing the proportion of free (unbound) fluorescent probe in the well, leading to low fluorescence polarization. Omission of enzyme (which gives the same result as use of a catalytically-dead enzyme) serves as a positive control. Compounds were tested at a nominal concentration of 5.9  $\mu$ M.

**Protocol Summary:** Prior to the start of the assay, Assay Buffer (4.0  $\mu$ L; 0.01% Pluronic acid, 50 mM Tris HCl pH 8.0, 150 mM NaCl, 1mM DTT) containing LYPLA1 protein (6.25 nM) was dispensed into 1536-well microtiter plates. Next, test compound (30 nL in DMSO) or DMSO alone (0.59% final concentration) was added to the appropriate wells and incubated for 30 minutes at 25 degrees Celsius. The assay was started by dispensing FP-Rh probe (1.0  $\mu$ L of 375 nM in Assay Buffer) to all wells. Plates were centrifuged and, after 10 minutes of incubation at 25 degrees Celsius, fluorescence polarization was read on a Viewlux microplate reader (PerkinElmer, Turku, Finland) using a BODIPY TMR FP filter set and a BODIPY dichroic mirror (excitation = 525 nm, emission = 598 nm). Fluorescence polarization was read for 15 seconds for each polarization plane (parallel and perpendicular). The well fluorescence polarization value (mP) was obtained via the PerkinElmer Viewlux software. **Assay Cutoff:** Compounds that inhibited LYPLA1 greater than 14.15% were considered active.

#### **Confirmation uHTS assay to identify LYPLA1 inhibitors (AID 2233)**

**Assay Overview:** The purpose of this assay was to confirm activity of compounds identified as active in the primary uHTS screen (AID 2174). In this assay, the FP-Rh probe was used to label LYPLA1 in the presence of test compounds and analyzed as described above (AID 2174). Compounds were tested in triplicate at a nominal concentration of 5.9  $\mu$ M.

**Protocol Summary:** The assay was performed as described above (AID 2174), except that compounds were tested in triplicate. **Assay Cutoff:** Compounds that inhibited LYPLA1 greater than 14.15% were considered active.

#### **Primary uHTS assay to identify LYPLA2 inhibitors (AID 2177)**

**Assay Overview:** The purpose of this assay was to identify compounds that act as LYPLA2 inhibitors. This assay also serves as a counterscreen for a set of previous experiments entitled, "Fluorescence polarization-based primary biochemical high throughput screening assay to identify inhibitors of Protein Phosphatase Methyltransferase 1 (PME-1)" (AID 2130). This competitive activity-based protein profiling (ABPP) assay uses fluorescence polarization to investigate enzyme-substrate functional interactions based on active site-directed molecular probes. A fluorophosphonate-rhodamine (FP-Rh) probe, which broadly targets enzymes from the SH family was used to label LYPLA2 in the presence of test compounds. The reaction was

excited with linear polarized light and the intensity of the emitted light was measured as the polarization value (mP). As designed, test compounds that act as LYPLA2 inhibitors will prevent LYPLA2-probe interactions, thereby increasing the proportion of free (unbound) fluorescent probe in the well, leading to low fluorescence polarization. Omission of enzyme (which gives the same result as use of a catalytically-dead enzyme) serves as a positive control. Compounds were tested at a nominal concentration of 5.9  $\mu$ M.

**Protocol Summary:** Prior to the start of the assay, Assay Buffer (4.0  $\mu$ L; 0.01% Pluronic acid, 50 mM Tris HCl pH 8.0, 150 mM NaCl, 1mM DTT) containing LYPLA2 protein (9.38 nM) was dispensed into 1536-well microtiter plates. Next, test compound (30 nL in DMSO) or DMSO alone (0.59% final concentration) was added to the appropriate wells and incubated for 30 minutes at 25 degrees Celsius. The assay was started by dispensing FP-Rh probe (1.0  $\mu$ L of 375 nM in Assay Buffer) to all wells. Plates were centrifuged and, after 10 minutes of incubation at 25 degrees Celsius, fluorescence polarization was read on a Viewlux microplate reader (PerkinElmer, Turku, Finland) using a BODIPY TMR FP filter set and a BODIPY dichroic mirror (excitation = 525 nm, emission = 598 nm). Fluorescence polarization was read for 15 seconds for each polarization plane (parallel and perpendicular). The well fluorescence polarization value (mP) was obtained via the PerkinElmer Viewlux software. **Assay Cutoff:** Compounds that inhibited LYPLA2 greater than 25.78% were considered active.

#### **Confirmation uHTS assay to identify LYPLA2 inhibitors (AID 2232)**

**Assay Overview:** The purpose of this assay was to confirm activity of compounds identified as active in the primary uHTS screen (AID 2177). In this assay, the FP-Rh probe was used to label LYPLA2 in the presence of test compounds and analyzed as described above (AID 2177). Compounds were tested in triplicate at a nominal concentration of 5.9  $\mu$ M.

**Protocol Summary:** The assay was performed as described above (AID 2177), except that compounds were tested in triplicate. **Assay Cutoff:** Compounds that inhibited LYPLA2 greater than 25.78% were considered active.

#### **Secondary Assays**

##### **Inhibition and selectivity of triazole urea library members (AID 504520)**

**Assay Overview:** The purpose of this assay is to determine whether powder samples of test compounds can inhibit ABHD11 in a complex proteomic lysate and to estimate compound selectivity in an activity-based proteomic profiling (ABPP) assay. In this assay, a complex proteome is incubated with test compound followed by reaction with a rhodamine-conjugated fluorophosphonate (FP-Rh) activity-based probe. The reaction products are separated by SDS-PAGE and visualized in-gel using a flatbed fluorescence scanner. The percentage activity remaining is determined by measuring the integrated optical density (IOD) of the bands. As designed, test compounds that act as ABHD11 inhibitors will prevent enzyme-probe interactions, thereby decreasing the proportion of bound fluorescent probe, giving lower fluorescence intensity in the band in the gel. Percent inhibition is calculated relative to a DMSO (no compound) control.

**Protocol Summary:** Soluble proteome (1 mg/mL in DPBS) of BW5147-derived murine T-cells was treated with 30 nM, 150 nM, or 750 nM of test compound (1  $\mu$ L of a 50x stock in DMSO). Test compounds were incubated for 30 minutes at 25 degrees Celsius (50  $\mu$ L reaction volume). FP-Rh (1  $\mu$ L of 50x stock in DMSO) was added to a final concentration of 2  $\mu$ M. The reaction was incubated for 30 minutes at 25 degrees Celsius, quenched with 2x SDS-PAGE loading buffer, separated by SDS-PAGE and visualized by in-gel fluorescent scanning. The percentage activity remaining was determined by measuring the integrated optical density of the target (ABHD11) and anti-target (platelet-activating factor acetylhydrolase type 2 [PAFAH2], esterase D/formylglutathione hydrolase [ESD], lysophospholipase 1 [LYPLA1], lysophospholipase 2 [LYPLA2]) bands relative to a DMSO-only (no compound) control. **Assay Cutoff:** Compounds with  $\geq$ 50% inhibition of ABHD11 at 150 nM were considered active.

#### **Inhibition of ABHD11 *in situ* (AID 504505)**

**Assay Overview:** The purpose of this assay is to determine whether or not powder samples of test compounds can inhibit ABHD11 activity *in situ*. In this assay, cultured BW5147-derived murine T-cells are incubated with test compound. Cells are harvested and the soluble fraction is isolated and reacted with a rhodamine-conjugated fluorophosphonate (FP-Rh) activity-based probe. The reaction products are separated by SDS-PAGE and visualized in-gel using a flatbed fluorescence scanner. The percentage activity remaining is determined by measuring the integrated optical density (IOD) of the bands. As designed, test compounds that act as ABHD11 inhibitors will prevent enzyme-probe interactions, thereby decreasing the proportion of bound fluorescent probe, giving lower fluorescence intensity in the band in the gel.

**Protocol Summary:** BW5147-derived murine T-cells (5 mL total volume; supplemented with FCS) were treated with 30 nM test compound (5  $\mu$ L of a 1000x stock in DMSO) for 4 hours at 37 degrees Celsius. Cells were harvested, washed 4 times with 10 mL DPBS, and homogenized by sonication in DPBS. The soluble fraction was isolated by centrifugation (100K x g, 45 minutes) and the protein concentration was adjusted to 1 mg/mL with DPBS. FP-Rh (1  $\mu$ L of 50x stock in DMSO) was added to a final concentration of 2  $\mu$ M in 50  $\mu$ L total reaction volume. The reaction was incubated for 30 minutes at 25 degrees Celsius, quenched with 2x SDS-PAGE loading buffer, separated by SDS-PAGE and visualized by in-gel fluorescent scanning. The percentage activity remaining was determined by measuring the integrated optical density of the ABHD11 band relative to a DMSO-only (no compound) control. **Assay Cutoff:** Compounds with  $\geq$ 90% inhibition of ABHD11 were considered active.

#### **Determination of IC50 values against ABHD11 *in vitro* (AID 504507)**

**Assay Overview:** The purpose of this assay is to determine the IC50 values of powder samples of test compounds for ABHD11 inhibition in a complex proteome lysate. In this assay, a fluorophosphonate-conjugated rhodamine (FP-Rh) activity-based probe is used to label ABHD11 in the presence of test compounds. The reaction products are separated by SDS-PAGE and visualized in-gel using a flatbed fluorescence scanner. The percentage activity remaining is determined by measuring the integrated optical density of the bands. As designed, test compounds that act as ABHD11 inhibitors will prevent enzyme-probe interactions, thereby



decreasing the proportion of bound fluorescent probe, giving lower fluorescence intensity in the band in the gel.

**Protocol Summary:** Soluble proteome (1 mg/mL in DPBS) of BW5147-derived murine T cells was incubated with DMSO or compound for 30 minutes at 25 degrees Celsius before the addition of FP-Rh at a final concentration of 2  $\mu$ M in 50  $\mu$ L total reaction volume. The reaction was incubated for 30 minutes at 25 degrees Celsius, quenched with 2x SDS-PAGE loading buffer, separated by SDS-PAGE and visualized by in-gel fluorescent scanning. The percentage activity remaining was determined by measuring the integrated optical density of the bands. IC50 values for inhibition of ABHD11 were determined from dose-response curves from three replicates at each inhibitor concentration (7-point 1:3 dilution series from 300 nM to 0.3 nM).

**Assay Cutoff:** Compounds with an IC50 < 100 nM were considered active.

#### **Determination of IC50 values against ABHD11 *in situ* (AID 504482)**

**Assay Overview:** The purpose of this assay is to determine the IC50 values of powder samples of test compounds for ABHD11 inhibition *in situ*. In this assay, cultured cells are incubated with test compound. Cells are harvested and the soluble fraction is isolated and reacted with a rhodamine-conjugated fluorophosphonate (FP-Rh) activity-based probe. The reaction products are separated by SDS-PAGE and visualized in-gel using a flatbed fluorescence scanner. The percentage activity remaining is determined by measuring the integrated optical density of the bands. As designed, test compounds that act as ABHD11 inhibitors will prevent enzyme-probe interactions, thereby decreasing the proportion of bound fluorescent probe, giving lower fluorescence intensity in the band in the gel.

**Protocol Summary:** BW5147-derived murine T cells (5 mL total volume; supplemented with 10% FCS) were treated with DMSO or test compound (5  $\mu$ L of a 1000x stock in DMSO) for 4 hours at 37 degrees Celsius. Cells were harvested, washed 4 times with 10 mL DPBS, and homogenized by sonication in DPBS. The soluble fraction was isolated by centrifugation (100K x g, 45 minutes) and the protein concentration was adjusted to 1 mg/mL with DPBS. FP-Rh (1  $\mu$ L of 50x stock in DMSO) was added to a final concentration of 2  $\mu$ M in 50  $\mu$ L total reaction volume. The reaction was incubated for 30 minutes at 25 degrees Celsius, quenched with 2x SDS-PAGE loading buffer, separated by SDS-PAGE and visualized by in-gel fluorescent scanning. The percentage activity remaining was determined by measuring the integrated optical density of the ABHD11 band relative to a DMSO-only (no compound) control. IC50 values for inhibition of ABHD11 were determined from dose-response curves from three replicates at each inhibitor concentration (4-point 1:3 dilution series from 2.5 nM to 75 pM).

**Assay Cutoff:** Compounds with an IC50 < 100 nM were considered active

#### **Analysis of Cytotoxicity (AID 504510)**

**Assay Overview:** The purpose of this assay is to determine cytotoxicity of inhibitor compounds belonging to the urea triazole scaffold. In this assay, BW5147-derived murine T-cells in either serum-free media (**Assay 1**) or media containing FCS (**Assay 2**) are incubated with test compounds, followed by determination of cell viability. The assay utilizes the WST-1 substrate that is converted into colorimetric formazan dye by the metabolic activity of viable cells. The

amount of formed formazan directly correlates to the number of metabolically active cells in the culture. As designed, compounds that reduce cell viability will result in decreased absorbance of the dye. Compounds were tested in quadruplicate in a 7-point 1:5 dilution series starting at a nominal test concentration of 50  $\mu$ M.

**Protocol Summary:** This assay was started by dispensing BW5147-derived murine T cells in RPMI media (100 $\mu$ L, 10E4 cells/well) into a 96-well plate. Both serum-free media (**Assay 1**) and media supplemented with fetal calf serum (FCS) (**Assay 2**) were tested. Compound (5  $\mu$ L of 0-1000  $\mu$ M in media containing 5% DMSO) was added to each well, giving final compound concentrations of 0-50  $\mu$ M. Cells were incubated for 48 hours at 37 degrees Celsius in a humidified incubator and cell viability was determined by the WST-1 assay (Roche) according to manufacturer instructions. **Assay Cutoff:** Compounds with a CC50 value of <5  $\mu$ M were considered active (cytotoxic).

### **LC-MS/MS Analysis of Inhibitor Binding Mode (AID 504498)**

**Assay Overview:** The purpose of this assay is to assess the covalent nature of an inhibitor compound belonging to the urea triazole scaffold and determine whether or not it labels the active site serine of ABHD11. In this assay, purified enzyme is reacted with inhibitor compound, digested with trypsin, and the resulting peptides are analyzed by liquid chromatography-tandem mass spectrometry (LC-MS/MS). The resulting data are analyzed to identify sites of covalent labeling.

**Protocol Summary:** Two aliquots (25  $\mu$ L) of 50  $\mu$ M ABHD11 were prepared. To one aliquot was added inhibitor (0.5  $\mu$ L of 10 mM in DMSO), giving a final concentration of 200  $\mu$ M. To the second (control) aliquot was added DMSO (0.5  $\mu$ L). Reactions were gently vortexed and incubated at room temperature for 30 minutes. To each reaction was added solid urea (50 mg), followed by freshly prepared aqueous ammonium bicarbonate (75  $\mu$ L of 25 mM). The reactions were vortexed until the urea was dissolved. Final urea concentration was approximately 8 M. To each reaction was added freshly prepared TCEP (5  $\mu$ L of 100 mM in water), and the reactions were incubated at 30 degrees C for 30 minutes. To each reaction was then added freshly prepared IAA (10  $\mu$ L of 100 mM in water), and the reactions were incubated for 30 min at room temperature in the dark. Aqueous ammonium bicarbonate (375  $\mu$ L of 25 mM) was added to reduce the urea concentration to 2 M. To each reaction was added sequencing grade modified trypsin (1  $\mu$ g), and reactions were incubated at 37 degrees C for 12 hours. Formic acid was added to 5% (v/v) final.

An Agilent 1200 series quaternary HPLC pump and Thermo Scientific LTQ-Orbitrap mass spectrometer were used for sample analysis. A fraction (10  $\mu$ L) of the protein digest for each sample was pressure-loaded onto a 100 micron fused-silica column (with a 5 micron in-house pulled tip) packed with 10 cm of Aqua C18 reversed-phase packing material. Chromatography was carried out using an increasing gradient of aqueous acetonitrile containing 0.1% formic acid over 125 minutes. Mass spectra were acquired in a data-dependent mode with dynamic exclusion enabled.

The MS/MS spectra generated for each run were searched against a human protein database concatenated to a reversed decoy database using Sequest. A static modification of +57.021

was specified for cysteine, and a variable modification of +139.100 was specified for serine to account for possible probe labeling by AA44-1. The resulting peptide identifications were assembled into protein identifications using DTASelect, and filters were adjusted to maintain a false discovery rate (as determined by number of hits against the reversed database) of <1%. Any modified peptides identified in the DMSO-treated sample were discarded as spurious hits. **Assay Cutoff:** Compounds observed to covalently modify the active site serine of ABHD11 were considered active.

### **SILAC-ABPP Analysis of Inhibition and Selectivity (AID 504522)**

**Assay Overview:** The purpose of this assay is to determine the selectivity profile of powder samples of test compounds using stable isotope labeling with amino acids in cell culture (SILAC) ABPP. In this assay, cultured BW5147-derived murine T-cells are metabolically labeled with light or heavy amino acids. Light and heavy cells are treated with inhibitor and DMSO, respectively, *in situ*. Cells are lysed, proteomes are treated with FP-biotin, and combined in a 1:1 (w/w) ratio. Biotinylated proteins are enriched, trypsinized, and analyzed by LC/LC-MS/MS (MudPIT). Inhibition of target and anti-target activity is quantified by comparing intensities of light and heavy peptide peaks. As designed, compounds that act as inhibitors will block FP-biotin labeling, reducing enrichment in the inhibitor-treated (light) sample relative to the DMSO-treated (heavy) sample, giving a smaller light/heavy ratio for each protein. Proteins not targeted by inhibitors would be expected to have a ratio of 1.

### **Protocol Summary:**

*Stable isotope labeling with amino acids in cell culture (SILAC).* BW5147-derived murine T-cell hybridoma cells were initially grown for 6 passages in either light or heavy SILAC RPMI 1640 media supplemented with 10% dialyzed FCS and 1x PenStrep Glutamine. Light media was supplemented with 100 µg/mL L-arginine (Sigma) and 100 µg/mL L-lysine (Sigma). Heavy media was supplemented with 100 µg/mL [<sup>13</sup>C<sub>6</sub><sup>15</sup>N<sub>4</sub>]-L-Arginine (Isotek) and 100 µg/mL [<sup>13</sup>C<sub>6</sub><sup>15</sup>N<sub>2</sub>]-L-Lysine (Isotek). Cells were treated with 3 nM test compound (5 µL of a 1000x stock in DMSO) for 4 hours at 37 degrees Celsius. Cells were harvested, washed 4 times with 10 mL DPBS, and homogenized by sonication in DPBS. The soluble and membrane fractions were isolated by centrifugation (100K x g, 45 minutes) and the protein concentration was adjusted to 1 mg/mL with DPBS.

*Sample preparation for ABPP-SILAC.* The light and heavy proteomes were labeled with 7 µM of FP-biotin (500 µL total reaction volume) for 1.5 hours at 25 degrees Celsius. After incubation, light and heavy proteomes were mixed in 1:1 ratio, and the membrane proteomes were additionally solubilized with 1% Triton-X100. The proteomes were desalted over PD-10 desalting columns (GE Healthcare) and FP-labeled proteins were enriched with streptavidin beads. The beads were washed with 1% SDS in PBS (1x), PBS (3x), and H<sub>2</sub>O (3x), then resuspended in 6 M urea, reduced with DTT for 15 minutes at 60 degrees Celsius, and alkylated with iodoacetamide for 30 minutes at 25 degrees Celsius in the dark. On-bead digestions were performed for 12 hours at 37 degrees Celsius with trypsin (Promega; 4 µL of 0.5 µg/µL) in the presence of 2 mM CaCl<sub>2</sub>. Peptide samples were acidified to a final concentration of 5% formic

acid, pressure-loaded on to a biphasic (strong cation exchange/reverse phase) capillary column and analyzed as described.

**LC-MS/MS analysis.** Digested and acidified peptide mixtures were analyzed by two-dimensional liquid chromatography (2D-LC) separation in combination with tandem mass spectrometry using an Agilent 1100-series quaternary pump and Thermo Scientific LTQ Orbitrap ion trap mass spectrometer. Peptides were eluted in a 5-step MudPIT experiment using 0%, 25%, 50%, 80%, and 100% salt bumps of 500 mM aqueous ammonium acetate and data were collected in data-dependent acquisition mode with dynamic exclusion turned on (60 s, repeat of 1). Specifically, one full MS (MS1) scan (400-1800 m/z) was followed by 7 MS2 scans of the most abundant ions. The MS2 spectra data were extracted from the raw file using RAW Xtractor (version 1.9.1; publicly available at <http://fields.scripps.edu/?q=content/download>). MS2 spectra data were searched using the SEQUEST algorithm (Version 3.0) against the latest version of the mouse IPI database concatenated with the reversed database for assessment of false-discovery rates. SEQUEST searches allowed for variable oxidation of methionine (+16), static modification of cysteine residues (+57 due to alkylation), and no enzyme specificity. The resulting MS2 spectra matches were assembled into protein identifications and filtered using DTASelect (version 2.0.41) using the --trypstat option, which applies different statistical models for the analysis of tryptic, half-tryptic, non-tryptic peptides. DTASelect 2.0 uses a quadratic discriminant analysis to achieve a user-defined maximum peptide false positive rate; the default parameters (maximum false positive rate of 2%) was used for the search; however, the actual false positive rate was much lower (1%). Ratios of Light/Heavy peaks were calculated using in-house software; reported ratios represent the mean of all unique, quantified peptides per protein. **Assay Cutoff:** A compound was considered active for a particular target/anti-target with a light/heavy ratio of  $\leq 0.5$

### **Inhibition of human ABHD11 *in vitro* (AID 504892)**

**Assay Overview:** The purpose of this assay is to determine whether powder samples of test compounds can inhibit the human isoform of ABHD11 in a complex proteomic lysate. In this assay, a complex proteome containing recombinant human ABHD11 is incubated with test compound followed by reaction with a rhodamine-conjugated fluorophosphonate (FP-Rh) activity-based probe. The reaction products are separated by SDS-PAGE and visualized in-gel using a flatbed fluorescence scanner. The percentage activity remaining is determined by measuring the integrated optical density (IOD) of the bands. As designed, test compounds that act as ABHD11 inhibitors will prevent enzyme-probe interactions, thereby decreasing the proportion of bound fluorescent probe, giving lower fluorescence intensity in the band in the gel. Percent inhibition is calculated relative to a DMSO (no compound) control.

**Protocol Summary:** Recombinant human ABHD11 (50  $\mu\text{g}/\text{mL}$ ) was spiked into mouse brain membrane proteome (1 mg/mL in DPBS, 50  $\mu\text{L}$  reaction volume) and treated with 0 (DMSO only), 3, 10, 30, or 150 nM or 20  $\mu\text{M}$  test compound (1  $\mu\text{L}$  of a 50x stock in DMSO). (Note: mouse membrane proteome alone is used as a control for visualization and quantification of the human ABHD11 band). Test compounds were incubated for 30 minutes at 25 degrees Celsius. FP-Rh (1  $\mu\text{L}$  of 50x stock in DMSO) was added to a final concentration of 2  $\mu\text{M}$ . The reaction was incubated for 30 minutes at 25 degrees Celsius, quenched with 2x SDS-PAGE loading

buffer, separated by SDS-PAGE and visualized by in-gel fluorescent scanning. The percentage activity remaining was determined by measuring the integrated optical density of the human ABHD11 band. **Assay Cutoff:** Compounds with  $\geq 50\%$  inhibition of ABHD11 at 30 nM were considered active.

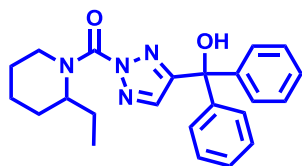
**Table 1** gives an overview of the PubChem assays associated with the LYPLA1 inhibitor project and indicates which are associated with the current probe development effort for **ML226**.

**Table 1.** Overview of PubChem assays for the LYPLA1 inhibitor project.

AID	Assay Name	Tested/ Active	Non- ML Tested	Purch Tested/ Active	Synth Tested/ Active
AID 2174	Counterscreen for PME1 inhibitors: fluorescence polarization-based primary biochemical high throughput screening assay to identify inhibitors of lysophospholipase 1 (LYPLA1) <i>LYPLA1/LYPLA2 dual inhibitor probe report (ML211)</i>	315002/499	0	0	0
AID 2233	Counterscreen for PME1 inhibitors: fluorescence polarization-based biochemical high throughput confirmation assay for inhibitors of lysophospholipase 1 (LYPLA1) <i>LYPLA1/LYPLA2 dual inhibitor probe report (ML211)</i>	478/331	0	0	0
AID 2177	Counterscreen for PME1 inhibitors: fluorescence polarization-based primary biochemical high throughput screening assay to identify inhibitors of lysophospholipase 2 (LYPLA2) <i>LYPLA1/LYPLA2 dual inhibitor probe report (ML211)</i>	315002/1197	0	0	0
AID 2232	Counterscreen for PME1 inhibitors: fluorescence polarization-based biochemical high throughput confirmation assay to identify inhibitors of lysophospholipase 2 (LYPLA2) <i>LYPLA1/LYPLA2 dual inhibitor probe report (ML211)</i>	1098/790	0	0	0
AID 493105	Assay provider results from the probe development effort to identify dual inhibitors of LYPLA1 and LYPLA2: Fluorescence-based biochemical gel-based ABPP inhibition of recombinant and endogenous enzyme <i>LYPLA1/LYPLA2 dual inhibitor probe report (ML211)</i>	91/29	0	0	0
AID 493111	Late stage assay provider results from the probe development effort to identify dual inhibitors of LYPLA1 and LYPLA2: Fluorescence-based biochemical gel-based ABPP inhibition and selectivity <i>LYPLA1/LYPLA2 dual inhibitor probe report (ML211)</i>	20/7	19	0/0	19/7
AID 493108	Late stage assay provider results from the probe development effort to identify dual inhibitors of LYPLA1 and LYPLA2: fluorescence-based cell-based inhibition <i>LYPLA1/LYPLA2 dual inhibitor probe report (ML211)</i>	3/2	3	0/0	3/2
AID 493110	Late stage assay provider results from the probe development effort to identify dual inhibitors of LYPLA1 and LYPLA2: Gel-based Activity-Based Protein Profiling (ABPP) IC50 for LYPLA1 and LYPLA2 <i>LYPLA1/LYPLA2 dual inhibitor probe report (ML211)</i>	5/3	5	0/0	5/3
AID 493154	Late stage assay provider results from the probe development effort to identify inhibitors of LYPLA1 and LYPLA2: Gel-based Activity-Based Protein Profiling (ABPP) IC50 for off-target ABHD11 <i>LYPLA1/LYPLA2 dual inhibitor probe report (ML211)</i>	2/2	2	0/0	2/2

AID 493161	Late stage assay provider results from the probe development effort to identify dual inhibitors of LYPLA1 and LYPLA2: absorbance-based cell-based dose response assay to determine cytotoxicity of inhibitor compounds <i>LYPLA1/LYPLA2 dual inhibitor probe report (ML211)</i>	3/0	3	0/0	3/0
AID 493109	Late stage assay provider results from the probe development effort to identify dual inhibitors of LYPLA1 and LYPLA2: LC-MS/MS assay to assess binding of compounds to active site <i>LYPLA1/LYPLA2 dual inhibitor probe report (ML211)</i>	1/1	1	0/0	1/1
<b>The following AIDs are for the new current probe development effort (ML226)</b>					
AID 504520	Late stage assay provider results from the probe development effort to identify inhibitors of LYPLA1: fluorescence-based biochemical gel-based Activity-Based Protein Profiling (ABPP) inhibition and selectivity	20/6	20	0/0	20/6
AID 504505	Late stage assay provider results from the probe development effort to identify inhibitors of LYPLA1: fluorescence-based cell-based gel-based Activity-Based Protein Profiling (ABPP) percent inhibition for anti-target ABHD11	1/1	1	0/0	1/1
AID 504507	Late stage assay provider results from the probe development effort to identify inhibitors of LYPLA1: fluorescence-based biochemical gel-based Activity-Based Protein Profiling (ABPP) IC50 for anti-target ABHD11 Set 2	3/3	3	0/0	3/3
AID 504482	Late stage assay provider results from the probe development effort to identify inhibitors of LYPLA1: fluorescence-based cell-based gel-based Activity-Based Protein Profiling (ABPP) IC50 for anti-target ABHD11	2/2	2	0/0	2/2
AID 504510	Late stage assay provider results from the probe development effort to identify inhibitors of LYPLA1: absorbance-based cell-based dose response assay to determine cytotoxicity of inhibitor compounds set 2	2/0	2	0/0	2/0
AID 504498	Late stage assay provider results from the probe development effort to identify inhibitors of LYPLA1: LC-MS/MS assay to assess binding of compounds to active site of anti-target ABHD11	1/1	1	0/0	1/1
ADI 504522	Late stage assay provider results from the probe development effort to identify inhibitors of LYPLA1: LC-MS-based cell-based SILAC Activity-Based Protein Profiling (ABPP) for anti-target ABHD11	1/1	1	0/0	1/1
AID 504892	Late stage assay provider results from the probe development effort to identify inhibitors of ABHD11: Fluorescence-based biochemical gel-based Activity-Based Protein Profiling (ABPP) inhibition of the human isoform of ABHD11	2/1	2	0/0	2/1

## 2.2 Probe Chemical Characterization



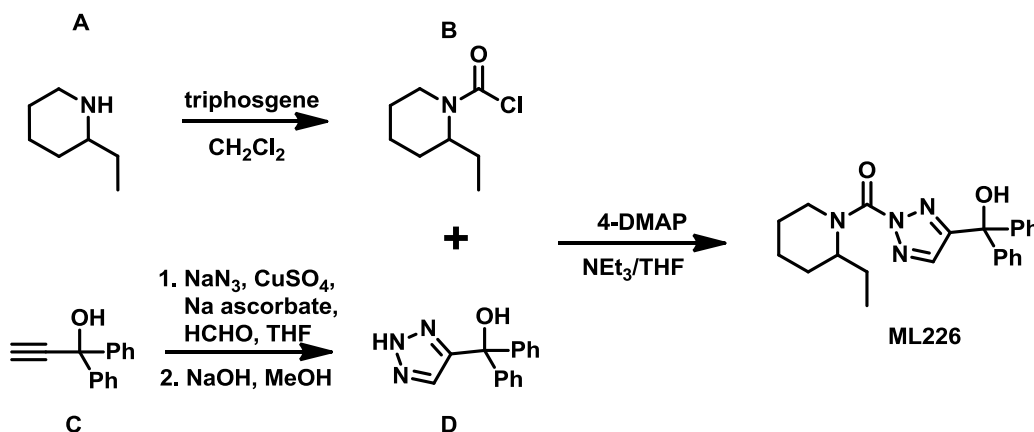
CID 56593112  
SID 99445332  
ML226

The probe structure was verified by  $^1\text{H}$  NMR (see **section 2.3**) and high resolution MS ( $m/z$  calculated for  $\text{C}_{23}\text{H}_{26}\text{N}_4\text{O}_2$   $[\text{M}+\text{H}]^+$ : 390.2056; found: 390.2053). Purity was assessed to be greater than 95% by NMR. The 2,4-regiochemistry was assigned by NMR by comparison with NMR shifts of triazole urea compounds of known 1,4 and 2,4 triazole substitution based on crystal structure data [12]. Solubility in PBS at room temperature was determined by UV trace to be  $27\ \mu\text{M}$  and stability in PBS was determined by LC-MS to be  $>48$  hours.

**Table 2.** Compounds submitted to the SMR collection.

Designation	CID	SID	SRID	MLS
Probe	56593112	99445332	SR-02000000952-1	MLS003448140
Analog 1	50904525	110923249	SR-02000001127-1	MLS003448141
Analog 2	50904527	110923252	SR-02000001130-1	MLS003448142
Analog 3	50904528	110923256	SR-02000001134-1	MLS003448143
Analog 4	46937241	99445330	SR-02000000950-1	MLS003448144
Analog 5	50904531	110923253	SR-02000001131-1	MLS003448145

## 2.3 Probe Preparation



*Synthesis of 2-ethylpiperidine-1-carbonyl chloride (B), racemic mixture:* 2-ethylpiperidine **A** (1 equiv) was dissolved in dry  $\text{CH}_2\text{Cl}_2$  (10 mL/mmol) and cooled to 0 degrees Celsius. Triphosgene (0.6 equiv) was added and the reaction was stirred for 10 minutes at 0 degrees Celsius and for further 15 minutes at room temperature. The reaction was carefully quenched by dropwise

addition of saturated aqueous NaHCO<sub>3</sub>, diluted with CH<sub>2</sub>Cl<sub>2</sub> and washed with brine. The organic phase was dried over Na<sub>2</sub>SO<sub>4</sub> and the solvent was removed under reduced pressure (water bath temperature <30 degrees Celsius). The crude carbamoyl chloride **B** was used for the next step without further purification. **CAUTION:** *Triphosgene is very toxic. This reaction should be performed in a well-ventilated fume hood. Any object that comes into contact with triphosgene should be rinsed with 10% NaOH solution.*

*Synthesis of diphenyl(1H-1,2,3-triazol-4-yl)methanol (D):* NH-1,2,3-triazole **D** was prepared following a slightly modified procedure of Fokin *et al.* [17]. A mixture of 37% HCHO (10 equiv), glacial AcOH (1.5 equiv), and THF (1 mL/mmol **C**) was stirred for 15 minutes. Sodium azide was added (1.5 equiv), followed by 1,1-diphenyl-2-propyn-1-ol **C** (562 mg, 2.7 mmol, 1 equiv). The mixture was stirred for 10 minutes and sodium ascorbate (0.2 equiv) was added, followed by CuSO<sub>4</sub> solution (200 mg/mL H<sub>2</sub>O; 5 mol %). The reaction was stirred for 24 hours at 60 degrees Celsius. The solvents were removed and the residue was re-dissolved in 3:1 MeOH/2N NaOH (1 mL/mmol **C**). After stirring for 24 hours at room temperature, the solvents were azeotropically removed and the residue was purified by silica gel chromatography (15:85:1 MeOH/CH<sub>2</sub>Cl<sub>2</sub>/NEt<sub>3</sub>) to yield diphenyl(1H-1,2,3-triazol-4-yl)methanol **D** (495 mg, 2.0 mmol, 73%). <sup>1</sup>H-NMR (400 MHz, *d*<sub>6</sub>-DMSO): δ = 7.82 (s, 1H), 7.54-7.27 (m, 10H). HRMS: *m/z* calculated for C<sub>15</sub>H<sub>14</sub>N<sub>3</sub>O [M+H]<sup>+</sup>: 252.1131; found: 252.1135. **CAUTION:** *This reaction may result in the formation of hydrazoic acid and should be performed in a well-ventilated fume hood and behind a blast shield. Sodium azide should not be mixed with strong acids.*

*Synthesis of (2-ethylpiperidin-1-yl)(4-(hydroxydiphenylmethyl)-2H-1,2,3-triazol-2-yl) methanone (ML226), racemic mixture:* A mixture of carbonyl chloride **B** (135 mg, 0.77 mmol, 1 equiv), NH-1,2,3-triazole **D** (232 mg, 0.92 mmol, 1.2 equiv), and 4-DMAP (cat) in 5:1 THF/NEt<sub>3</sub> (2 mL/mmol **B**) was stirred for 10 hours at 60 degrees Celsius. The solvents were removed to yield the crude triazole urea **ML226** as a 3:1 mixture of *N*2- and *N*1-carbamoylated regioisomers. Regioisomers were easily distinguishable by <sup>1</sup>H-NMR shift of the triazole ring proton by comparison to NMRs for urea triazoles of known regiochemistry based on solved crystal structures [12]. The *N*2-carbamoyl triazole was isolated by silica gel chromatography (3:1 hexanes/ethyl acetate -> ethyl acetate) to afford pure **ML226** (132 mg, 0.34 mmol, 51% yield overall). <sup>1</sup>H-NMR (400 MHz, CDCl<sub>3</sub>): δ = 7.52 (s, 1H), 7.35-7.23 (m, 10H), 3.68-3.12 (m, 3H), 1.87-1.16 (m, 8H), 0.81 (m, 3H), purity >95%. HRMS: *m/z* calculated for C<sub>23</sub>H<sub>26</sub>N<sub>4</sub>O<sub>2</sub> [M+H]<sup>+</sup>: 390.2056; found: 390.2053.

### 3 Results

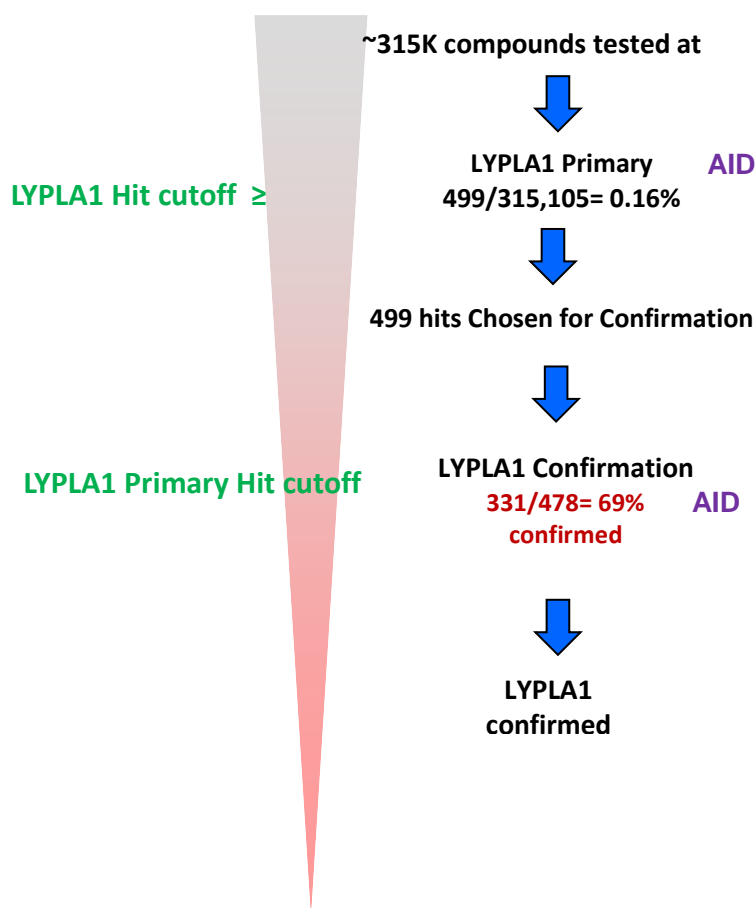
Probe **ML226** (Compound **12**, **SAR Table 4**) has an IC<sub>50</sub> value of 15 nM vs. ABHD11 and selectivity of ≥100 fold vs. more than 20 SHs (IC<sub>50</sub> ≥ 1500 nM; see **Section 3.2**). Potency and selectivity were confirmed by SILAC-ABPP (see **Section 3.6**). **ML226** was also shown to be highly active *in situ* against ABHD11 (see **Section 3.5**).



### 3.1 Summary of Screening Results

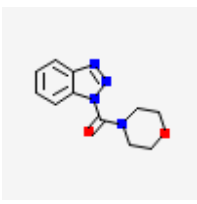
In the primary FluoPol HTS assay for LYPLA1 (AID 2174), ~315K compounds were screened with the SH-specific FP-Rh activity-based probe [10]. A total of 499 compounds (0.16%) were active, passing the set threshold of 14.15% LYPLA1 inhibition. For the confirmation HTS screen (AID 2233), 478 active compounds were retested in triplicate, and 331 compounds (69%) were confirmed as active (**Figure 1**). Prior to secondary screening, the active compounds were filtered to remove compounds with at least 30% activity against previous FluoPol ABPP enzyme inhibitor screens: GSTO1 (AID 1974; 48 compounds), FAM108b (AID 1947, 14 compounds), and PME-1 (AID 2130, 16 compounds). Additionally, 23 compounds with greater than 5% hit rate in all bioassays tested were removed, as well as the majority of compounds (30) that contained esters. Of the remaining 200 compounds, all hits with at least 50% inhibition against LYPLA1 (37 compounds) were chosen for secondary screening along with 54 additional compounds cherry-picked from the remaining hits (total compounds for secondary screening = 91). Of these 91 hits, the majority (62) also showed activity against LYPLA2 in the primary (AID 2177) and/or confirmation (AID 2232) FluoPol ABPP HTS assay for LYPLA2 inhibitors (activity cutoff: 25.78% inhibition).

The 91 compounds selected for secondary screening were assayed for their ability to inhibit both the recombinant human (rh) and endogenous mouse (em) isoforms of LYPLA1 and LYPLA2 by gel-based competitive ABPP in the context of a complex proteome (AID 493105; See Supplemental **Figures S1, S2, S3** of **ML211** Probe Report). Compounds with at least 30% inhibition were scored as active. In this assay, a complex proteome, containing endogenous and spiked-in recombinant forms of LYPLA1 or LYPLA2, is incubated with test compound (20  $\mu$ M) followed by reaction with a rhodamine-conjugated fluorophosphonate (FP-Rh) activity-based probe. The reaction products are separated by SDS-PAGE and visualized in-gel using a flatbed fluorescence scanner. Test compounds that act as



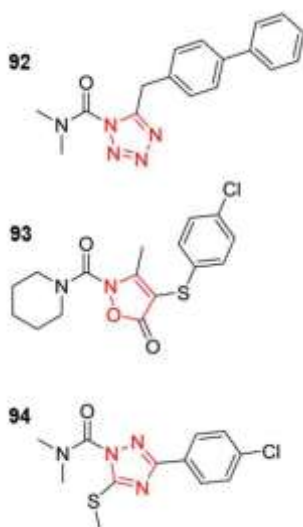
**Figure 1.** Flow chart describing HTS results.

LYPLA1/LYPLA2 inhibitors will prevent enzyme-probe interactions, thereby decreasing the fluorescence intensity of the protein bands. Nineteen compounds were active against rhLYPLA1, 10 compounds were active against rhLYPLA2, and 5 compounds were active against both human enzymes. Of the five compounds active against both rhLYPLA1 and rhLYPLA2, three were also active against emLYPLA1 and emLYPLA2. The top lead (SID 7974398, CID 735660, **Table 3**) has a triazole urea scaffold that appeared readily amenable to medchem optimization.

<b>Table 3.</b> Top HTS Hit from LYPLA1 Inhibitor Discovery Campaign.					
SID 7974398 CID 735660		% Inhibition (20 μM)			
		rhLYPLA1	rhLYPLA2	emLYPLA1	emLYPLA2
		98%	76%	99%	88%

Additionally, as discussed in ref. [12], while previously characterizing agents that perturb endocannabinoid uptake and metabolism, we discovered that the tetrazole urea LY2183240 (**92**, **Figure 2**) [18] was a potent inhibitor of numerous SHs [19], including the endocannabinoid-degrading enzymes fatty acid amide hydrolase (FAAH), monoacylglycerol lipase (MAGL or MGLL), and alpha/beta-hydrolase 6 (ABHD6), and have confirmed that **92** inhibits FAAH by covalent carbamoylation of the enzyme's serine nucleophile [19]. There are a handful of other reports of N-heterocyclic ureas as SH inhibitors, including the isoxazolonyl urea **93** [20] and 1,2,4-triazole urea **94** [21], which are potent inhibitors of hormone-sensitive lipase (LIPe); however, selectivity profiles have not been reported. Taken together, these data indicate that the triazole urea scaffold might be tolerant to modification without complete loss of binding efficiency, and would yield a probe with good *in vitro* and *in situ* properties.

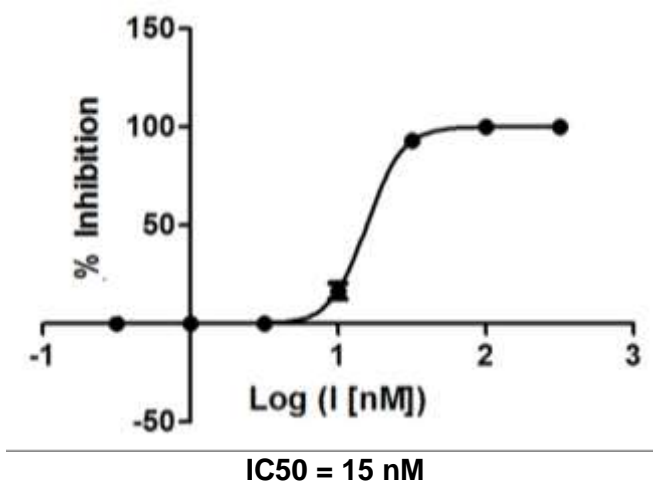
**Figure 2.** N-Heterocyclic Urea SH Inhibitors.



### 3.2 Dose Response Curves for Probe

IC50 values were obtained from gel-based competitive-ABPP data (**Figure 3**) as described in AID 504507.

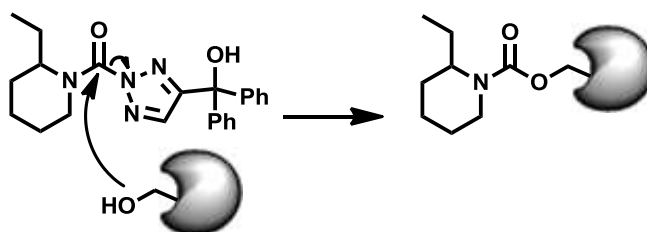
**Figure 3.** IC50 curve for probe **ML226** (compound **12**, SID 99445332) as determined by gel-based competitive-ABPP with FP-Rh (AID 504507) against target ABHD11 in a complex proteome lysate.



### 3.3 Scaffold/Moiety Chemical Liabilities

The probe compound was determined by LC-MS/MS to covalently modify the catalytic serine (Ser141) of ABHD11 (AID 504498). The observed mass shift of the active site peptide corresponds to the adduct depicted in **Figure 4**, formed by serine nucleophilic attack at the carbonyl followed by loss of the triazole moiety to carbamoylate the enzyme.

**Figure 4.** Covalent modification of ABHD11 by probe **ML226** (compound **12**, SID 99445332)



Active Site Peptide:  
R.NHGDSPHSPDMSYEIMSQLDQLDQLPQLGLVPCVVVGH**S**<sub>141</sub>MGGK.T

The probe compound showed no reactivity with glutathione (100  $\mu$ M), indicating that it is not generally cysteine reactive, but rather has a tempered electrophilicity and specific structural elements that direct reactivity towards ABHD11.

An irreversible probe has some distinct advantages over reversible analogs. Targets can be readily characterized by methods such as mass spectrometry and click chemistry-ABPP, required dosing is often lower, irreversible compounds are not as sensitive to pharmacokinetic parameters, and administration can induce long-lasting inhibition [22]. In the case of the EGFR inhibitor PD 0169414, its irreversibility and high selectivity were credited with producing prolonged inhibition of the target, alleviating concerns over short plasma half-lives and reducing the need for high peak plasma levels, thus minimizing potential nonspecific toxic effects [23].

Indeed, over a third of enzymatic drug targets are irreversibly inhibited by currently marketed drugs [24]. Examples of covalent enzyme-inhibitor pairs include serine type D-Ala-D-Ala carboxypeptidase, which is covalently modified by all B-lactam antibiotics, acetylcholinesterase, whose active site serine undergoes covalent modification by pyridostigmine, prostaglandin-endoperoxide synthase, which is the target of the ubiquitously prescribed aspirin, aromatase, which is irreversibly modified by exemestane, monoamine oxidase, which is covalently modified by L-deprenyl, thymidylate synthase, which is covalently modified by floxuridine, H<sup>+</sup>/K<sup>+</sup> ATPase, which undergoes covalent modification by omeprazole, esomeprazole, and lansoprazole, and triacylglycerol lipase, whose serine nucleophile is targeted by orlistat [24].

### 3.4 SAR Tables

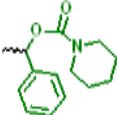
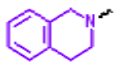
The SAR **Table 4** lists 34 triazole urea analogs, including the resynthesized triazole HTS hit (CID 735660, **Table 3**), which is listed as compound **1** (SID 92709166). The analogs are variable at three positions: the substituents of the urea nitrogen, **R**<sub>1</sub> and **R**<sub>2</sub>, and the substituent at 4-position of the triazole, **R**<sub>3</sub>. (Note: when the substituent of the urea nitrogen is a ring system, the group is denoted **R**<sub>1</sub>/**R**<sub>2</sub> in the SAR **Table 4** and the nomenclature includes the urea nitrogen.) The synthetic compounds were subject to gel-based competitive ABPP potency and selectivity analysis as outlined in AIDs 493111 and 504520 (see **Figures 7** and **8**) and summarized in SAR **Table 4**. As demonstrated for other triazole urea inhibitors [12], this type of gel-based competitive ABPP profiling allows for simultaneous assessment of both potency and selectivity of several dozen FP-sensitive SHs. As noted in SAR **Table 4A**, compounds **1-20** were analyzed at 30, 200, and 1500 nM concentration (**Figure 7**, see also **ML211** Probe Report), and compounds **21-34** (**Table 4B**) were analyzed at 30, 150, and 750 nM concentration (**Figure 8**). The only observed anti-targets up to 1500 nM (indicated by disappearance of band in compound-treated lane relative to the DMSO control) were N-acylaminoacyl-peptide hydrolase (APEH), platelet activating factor acetylhydrolase type II (PAFAH2), esterase D/formylglutathione hydrolase (ESD), lysophospholipase 1 (LYPLA1), and lysophospholipase 2 (LYPLA2).

Table 4A Target SAR Analysis*					Structure			Potency and Selectivity <sup>†</sup>								
					Entry	lab name	CID	SID	SRID	Regio-isomer	(R <sub>1</sub> /R <sub>2</sub> )**	R <sub>3</sub>	IC50 <i>in vitro</i> (nM) (AID 493154)	IC50 <i>in situ</i> (nM) (AID 504482)	% INH ABDH11 at given cpd conc. (AID 493111)	
30 nM	200 nM	1500 nM	30 nM	200 nM											1500 nM	
1	HTS hit	735660	92709166	SR-01000 625310-2	N1	morpholino	benzo <sup>††</sup>	18	ND	100	100	100			LYPLA1 ESD APEH	>11
2	AA26-5	46829228	99205814	SR-02000 000403-1	N1	morpholino	H	ND	ND	0	50	100				>7
3	AA34-1	46937239	99445324	SR-02000 000944-1	N2	morpholino	Ph	ND	ND	100	100	100		ESD APEH	ESD APEH	7
4	AA34-2	46937228	99445325	SR-02000 000945-1	N2	morpholino	3,5-difluoro Ph	ND	ND	100	100	100	APEH	ESD APEH	LYPLA1 ESD APEH	0
5	AA34-3	46937230	99445326	SR-02000 000946-1	N2	morpholino	4-OCF <sub>3</sub> Ph	ND	ND	100	100	100			ESD APEH	>6
6	AA34-4	46937235	99445327	SR-02000 000947-1	N2	morpholino	CPh <sub>2</sub> OH	ND	ND	100	100	100		LYPLA1	LYPLA1 LYPLA2 ESD APEH	>1
7	AA26-9	46829232	99205818	SR-02000 000407-1	N1	Piperidyl	H	ND	ND	0	50	100			LYPLA1	>1
8	AA40-1	46937232	99445331	SR-02000 000951-1	N2	Piperidyl	CPh <sub>2</sub> OH	ND	ND	100	100	100	LYPLA1	LYPLA1 LYPLA2 ESD	LYPLA1 LYPLA2 ESD APEH	0
9	AA40-2	46937234	99445328	SR-02000 000948-1	N2	Piperidyl	4-PhOPh	ND	ND	50	100	100	ESD	LYPLA1 ESD	LYPLA1 ESD	0
10	AA40-3	46937227	99445329	SR-02000 000949-1	N2	Piperidyl	6-OMe naphthal	ND	ND	50	100	100	ESD	ESD APEH	LYPLA1 LYPLA2 ESD APEH	0
11	AA47-1	46937241	99445330	SR-0200000095 0-1	N2	Piperidyl	CHPhOH	ND	ND	100	100	100	LYPLA1	LYPLA1 LYPLA2 ESD	LYPLA1 LYPLA2 ESD	0
12 (ML226)	AA44-1	56593112	99445332	SR-02000 000952-1	N2	2-Et piperidyl	CPh <sub>2</sub> OH	15	0.68	100	100	100			APEH	100

13	KLH31	46937238	99445333	SR-0200000953-1	N1	3-Bz piperidyl	CPh <sub>2</sub> OH	ND	ND	100	100	100	LYPLA1 LYPLA2	LYPLA1 LYPLA2	LYPLA1 LYPLA2 ESD	0
14	AA44-3	46937244	99445334	SR-0200000954-1	N2	4-Me piperidyl	CPh <sub>2</sub> OH	ND	ND	100	100	100	LYPLA1 LYPLA2	LYPLA1 LYPLA2 APEH	LYPLA1 LYPLA2 ESD APEH	0
15	AA49-1	46937233	99445335	SR-0200000955-1	N2	4-OMe piperidyl	CPh <sub>2</sub> OH	ND	ND	100	100	100	LYPLA1	LYPLA1 LYPLA2	LYPLA1 LYPLA2 ESD	0
16	AA50-1	46937231	99445336	SR-0200000956-1	N2	4-Bz piperidyl	CPh <sub>2</sub> OH	ND	ND	100	100	100	LYPLA1 LYPLA2	LYPLA1 LYPLA2	LYPLA1 LYPLA2 ESD	0
17	AA62-2	46937243	99445337	SR-0200000957-1	N2	4-CPh <sub>2</sub> OH piperidyl	CPh <sub>2</sub> OH	ND	ND	100	100	100	LYPLA1 LYPLA2	LYPLA1 LYPLA2	LYPLA1 LYPLA2	0
18 (ML211)	AA64-2	46937240	99445338	SR-0200000958-1	N2	4-tBu piperidyl	CPh <sub>2</sub> OH	10	ND	100	100	100	LYPLA1 LYPLA2	LYPLA1 LYPLA2	LYPLA1 LYPLA2 ESD	0
19	AA69-1	46937229	99445339	SR-0200000959-1	N2	4-tBu piperidyl	Cyclohexan (1)ol	ND	ND	100	100	100	LYPLA1	LYPLA1 LYPLA2	LYPLA1 LYPLA2 ESD	0
20	AA69-2	46937237	99445340	SR-0200000960-1	N2	4-tBu piperidyl	2-PrOH	ND	ND	0	0	100		LYPLA1 LYPLA2	LYPLA1 LYPLA2	0

Table 4B

Entry	lab name	CID	SID	SRID	Structure			IC50 <i>in vitro</i> (nM) (AID 504507)	IC50 <i>in situ</i> (nM) (AID 504482)	% INH ABDH11 at given cpd conc. (AID 504520)			Anti-target(s) <sup>‡</sup> (AID 504520)			Fold Selectivity <sup>§</sup> ABHD11 vs. other SHs (AID 504520)
					R <sub>1</sub>	R <sub>2</sub>	R <sub>3</sub>			30 nM	150 nM	750 nM	30 nM	150 nM	750 nM	
					(R <sub>1</sub> /R <sub>2</sub> )**											
21	KLH20	50904522	110923246	SR-0200001124-1	Ph	Ph	3,5-difluoro Ph	ND	ND	0	0	50			PAFAH2	0
22	KLH17	50904523	110923247	SR-0200001125-1	Ph	Ph	4-PhOPh	ND	ND	0	0	0			PAFAH2	ND
23	KLH21	50904524	110923248	SR-0200001126-1	Ph	Ph	4-biPh	ND	ND	0	0	0			PAFAH2	ND
24	KLH18	50904525	110923249	SR-0200001127-1	Ph	Ph	6-OMe naphthyl	ND	ND	0	0	25			PAFAH2	ND

25	KLH11	50904528	110923256	SR-02000 001134-1	Ph	Ph	C(iBu) <sub>2</sub> OH	ND	ND	0	0	50				>1
26	AA37-1	50904526	110923250	SR-02000 001128-1	Ph	Ph	CPh2OH	ND	ND	0	0	0				ND
27	AA37-2	50904532	110923251	SR-02000 001129-1	Ph	Me	CPh2OH	ND	ND	0	0	75				>1
28	KLH14	50904527	110923252	SR-02000 001130-1	Ph	3-bromo Ph	CPh2OH	ND	ND	0	100	100				>5
29	KLH13	50904529	110923254	SR-02000 001132-1	Ph	4-bromo Ph	CPh2OH	ND	ND	0	100	100				>5
30	KLH15	50904530	110923255	SR-02000 001133-1	Ph	2- naphthal	CPh2OH	ND	ND	0	100	100				>5
31	AA47-2	50918538	113234402	SR-02000 001137-1	Piperidyl			ND	ND	100	100	100	LYPLA1	LYPLA1 PAFAH2	LYPLA1 PAFAH2 ESD	0
32	AA51-1	50904531	110923253	SR-02000 001131-1			CPh2OH	ND	ND	100	100	100		PAFAH2	LYPLA1 PAFAH2	>1
33	AA43-1	50904533	110923257	SR-02000 001135-1	2-(3- methoxypropyl) piperidyl		CPh2OH	ND	ND	0	50	75				>5
34	AA44-2	49837808	103913583	SR-02000 001007-1	2-methoxymethyl piperidyl		CPh2OH	1	0.14	100	100	100				>750

\* All compounds listed are synthetic compounds

† Color scheme: green = active (IC<sub>50</sub>, inhibition data) or ≥5-fold selective (fold selectivity data)

grey = not determined (ND)

orange = one or more anti-target(s) with >50% INH

yellow = anti-target(s) with 50% INH

‡ Anti-targets: platelet-activating factor acetylhydrolase type 2 (PAFAH2), esterase D/formylglutathione hydrolase (ESD), lysophospholipases 1 and 2 (LYPLA1 and LYPLA2), N-acylaminoacyl-peptide hydrolase (APEH)

§ Fold selectivity:

--If in vitro IC<sub>50</sub> determined: fold selectivity = highest\_conc(≤50% INH anti-target) / IC<sub>50</sub>\_target

--If in vitro IC<sub>50</sub> not determined: fold selectivity = highest\_conc(≤50% INH anti-target) / lowest\_conc(≥50% INH target);

--If highest\_conc(≤50% INH anti-target) < lowest\_conc(≥50% INH target) fold selectivity = 0

\*\* Naming scheme for combined R1/R2 substituents (all cyclic) includes N

†† Fused at 5-position of triazole; see structure in Table 3

**SAR analysis of compounds 1-20:** Compounds **1-20** of **Table 4A** were initially synthesized during medchem optimization of a dual inhibitor for LYPLA1/LYPLA2 (**ML211**, compound **18**). With few exceptions (compounds **2**, **7**, **20**), all of these analogs are potent inhibitors of ABHD11, showing  $\geq 50\%$  enzyme inhibition at 30 nM compound concentration. As a class, these analogs had a small, cyclic substituent at  $R_1/R_2$  – morpholine or (substituted)piperidine – and a non-hydrogen moiety at  $R_3$ . Similarly, neither was 2-propanol tolerated as a substituent at  $R_3$  (compound **20**). ABHD11 appeared to tolerate a wide variety of functional groups at  $R_3$  – from the fused benzo substituent of the HTS hit (compound **1**) to large naphthyl (compound **10**) and diphenylmethanol (compounds **6**, **8**, **12-18**) groups – and diverse functionalization of the piperidine ring of  $R_1/R_2$  – from hydrogen (compounds **8-11**) to alkyl and/or aromatic groups of varying size at all three ring positions (compounds **12-19**). While this series showed great potency for ABHD11 inhibition, selectivity vs. other SHs was a significant problem for all analogs (see anti-target list, **Table 4**) with the sole exception of **ML226** (compound **12**). The unique feature of **ML226** was the location of its ethyl substituent at the 2-position of the piperidine ring. In previous studies, we have identified selective, moderate potency ( $IC_{50}$  values of  $\sim 100-200$  nM) carbamate inhibitors of ABHD11 that similarly possess a 2-substituted piperidine group [14] (see **section 4.1** for further discussion), indicating that selectivity may be derived in large part by this structural feature. **ML226** was  $\sim$ equipotent to the initial HTS hit (compound **1**), but appeared to be more selective, inhibiting only one anti-target at 1500 nM (APEH, 50% inhibition), whereas compound **1** showed reactivity with three anti targets: LYPLA1, ESD, and APEH at the same concentration. It should be noted that **ML226** was synthesized in racemic form, and the independent activity of each enantiomer has not yet been evaluated. Future work may address this issue through the design of a chiral synthetic route or via chiral separation of the two enantiomers.

**SAR analysis of compounds 21-34:** Following report of compound **12** as the anti-probe for LYPLA1/2 dual inhibitor **ML211**, we further explored SAR around ABHD11 with several additional compounds (**Table 4B**). To examine substitution at the 2-position, we synthesized compounds **33** and **34**, with 3-methoxypropyl and methoxymethyl groups at the 2-position, respectively. Compound **33** was less potent than **ML226**; however, compound **34** was found to be even more potent and selective than **ML226** ( $IC_{50} = 1$  nM, selectivity  $>750$ ), and could serve as a probe compound as well for ABHD11. (Note: compound **34** was not designated as the probe for consistency with the anti-probe reported in the **ML211** probe report).

We also investigated some more substantial structural modifications with compounds **21-32**. Instead of the cyclic piperidine, we synthesized compounds **21-26** where  $R_1=R_2$ =phenyl in combination with several different  $R_3$  groups, including preservation of diphenylmethanol (compound **26**) of **ML226**. However, all compounds showed negligible inhibition of ABHD11. Some potency was restored with the introduction of a halogen (bromine) at the 3 or 4 position of one of the phenyl rings (compounds **28** and **29**) or replacement of a phenyl with a naphthyl group (compound **30**). Interestingly, the phenyl series, while not being as potent for ABHD11, also did not show any evidence of anti-target reactivity, indicating that the structure is somewhat more privileged than many of the more promiscuous morpholine and piperidine compounds. Adding a fused benzene ring to the piperidine (compound **32**) gave the characteristic high potency/low selectivity signature of the other piperidine derivatives.

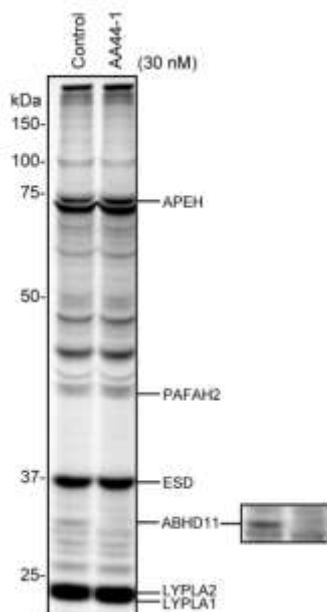


**Summary:** Overall, it appears that the general potency of the piperidine derivatives can be tempered by introduction of a small alkyl (ethyl, **ML226**) or alkoxyalkyl (methoxymethyl, compound **34**) substituent at the 2-position, rendering the resulting compounds uniquely selective for ABHD11. Future directions in SAR analysis will be a more in-depth exploration of the tolerance for diverse groups at the 2-position of the piperidine, combination with more diverse  $R_3$  groups, as well as addressing the independent activity of the two enantiomers of **ML226**.

### 3.5 Cellular Activity

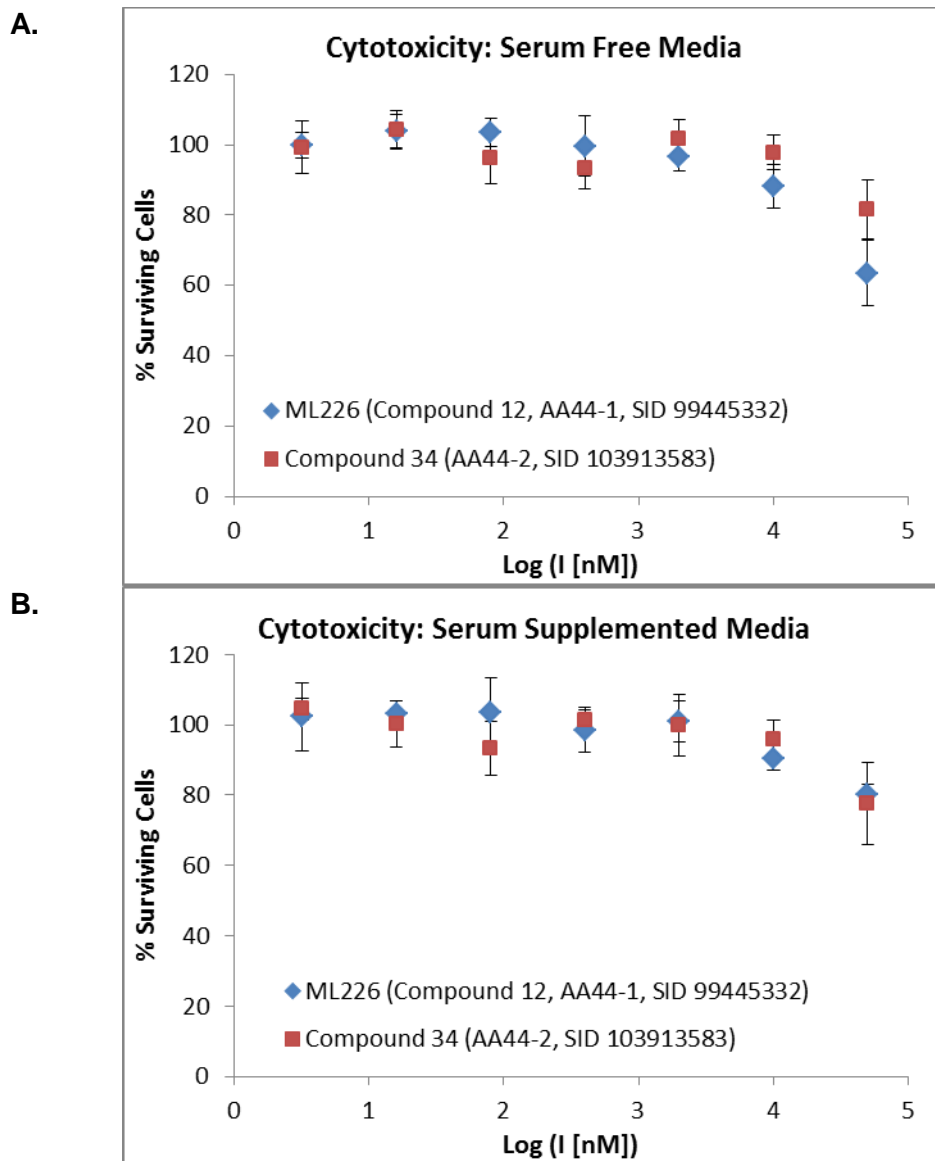
**In Situ Activity:** Probe **ML226** (Compound **12**, AA44-1) is highly active against ABHD11 *in situ* (AID 504505), completely inhibiting enzymatic activity at 30 nM compound concentration after 4 hours (media + 10% fetal calf serum) as assayed by gel-based competitive ABPP (**Figure 5**). The *in situ* IC<sub>50</sub> was determined to be 0.68 nM (AID 504482). This result indicates that **ML226** is free to cross cell membranes and inhibit its target in the cytoplasm of cells, even in the presence of serum-containing medium.

**Figure 5.** Selective inhibition of ABHD11 activity *in situ* by probe **ML226** (compound **12**, **AA44-1**, SID 99445332). Box at right shows darker image around ABHD11 band. Fluorescent image shown in grey scale.



**Cytotoxicity:** The probe **ML226** (compound **12**) and analog **34** were evaluated for cytotoxicity (AID 504510) using both serum-free and serum-supplemented media. As shown in **Figure 6**, both compounds have a CC<sub>50</sub> greater than 50  $\mu$ M, which is over 1500-fold greater than the concentration (30 nM) necessary for complete inhibition of ABHD11 *in situ*.

**Figure 6.** Cytotoxicity of probe **ML226** and analog **34** in serum-free (**A**) and serum-supplemented (**B**) media. See AID 504510 for details.



Outcome:	Compound	CC50 (serum free)	CC50 (serum supplemented)
	Probe <b>ML226</b>	>50 $\mu$ M	>50 $\mu$ M
	Compound <b>34</b>	>50 $\mu$ M	>50 $\mu$ M

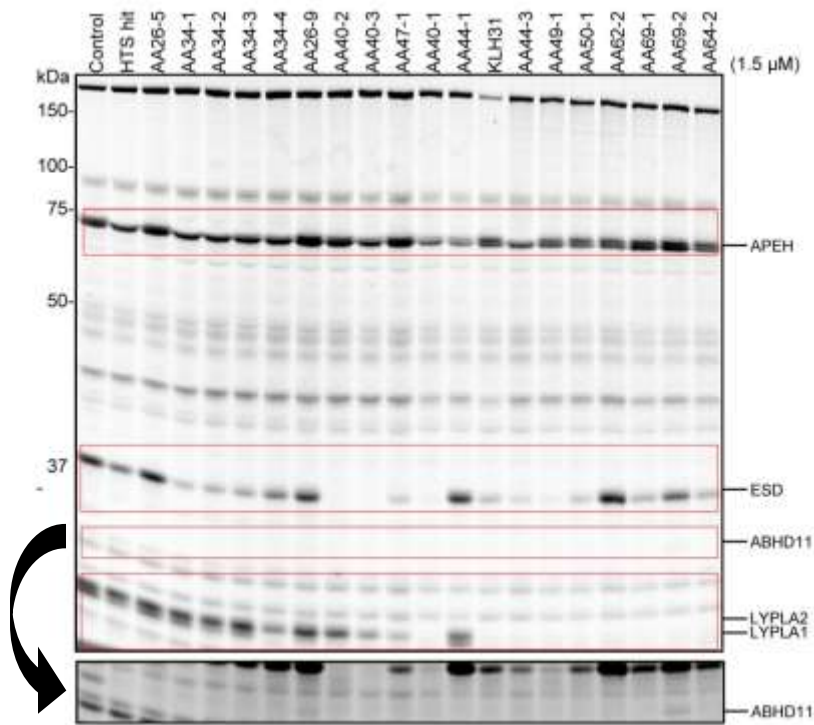
### 3.6 Profiling Assays

**HTS Assays:** To date, the HTS hit (Compound 1, CID 735660) has been tested in 504 other cell-based and non-cell-based bioassays deposited in PubChem, and has shown activity in only 11 of those assays, giving a hit rate of 2.0 %. This low hit rate indicates that this compound class may not be generally active. No HTS activity data is yet available for probe **ML226** (compound 12) or any of the synthetic analogs.

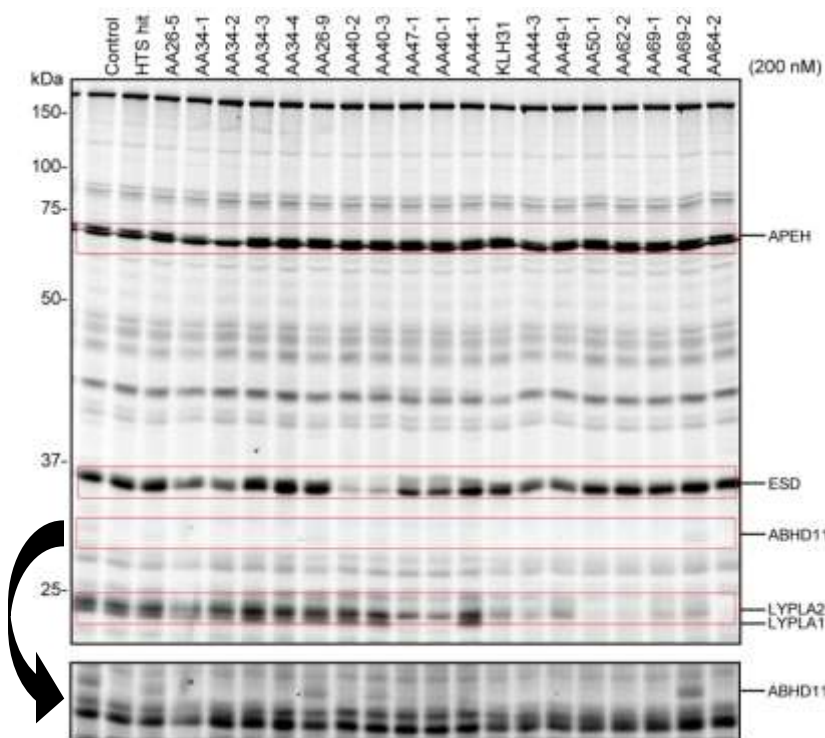
**Gel-Based Competitive ABPP:** Probe **ML226** and analogs listed in **Table 4** have been subject to gel-based competitive ABPP screening to assess SH reactivity. Competitive ABPP (**Figures 7 and 8**) was utilized for medchem optimization, allowing rapid assessment of anti-target inhibition (as visualized by disappearance of bands in compound-treated lanes) of analogs against >20 distinct SHs. The optimized probe **ML226** shows 100-fold selectivity against its nearest anti-target, APEH (50% inhibited at 1500 nM), and >100 fold selectivity against all other FP-sensitive SHs (**Figure 7A**, compound **AA44-1**, see also AID 493111).

**Figure 7.** Potency and selectivity of triazole urea synthetic library compounds **1-20** at three compound concentrations: 1.5  $\mu$ M (**A**), 200 nM (**B**), and 30 nM (**C**).

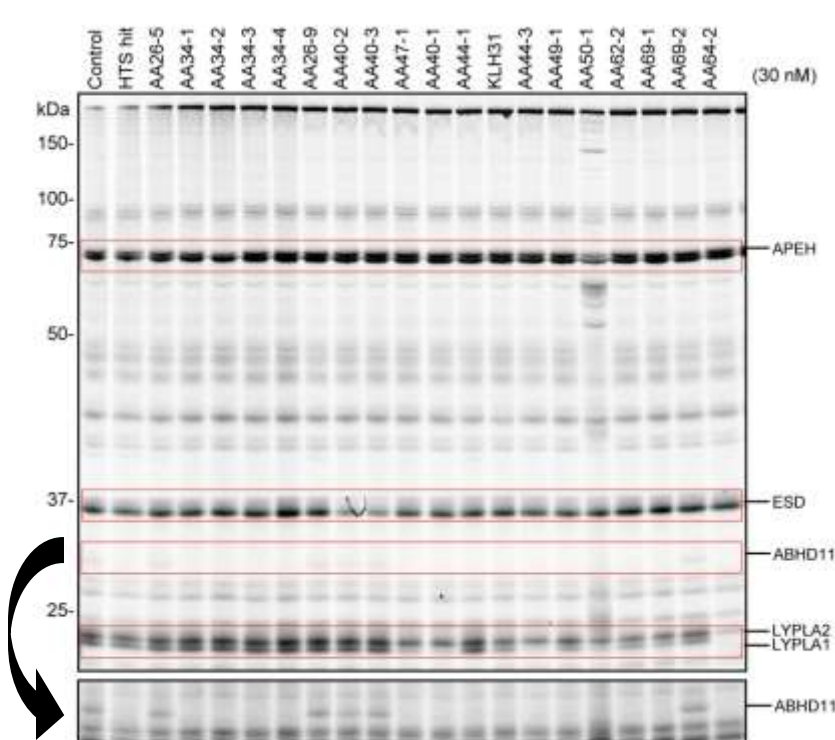
**A. 1.5  $\mu$ M**



**B. 200 nM**



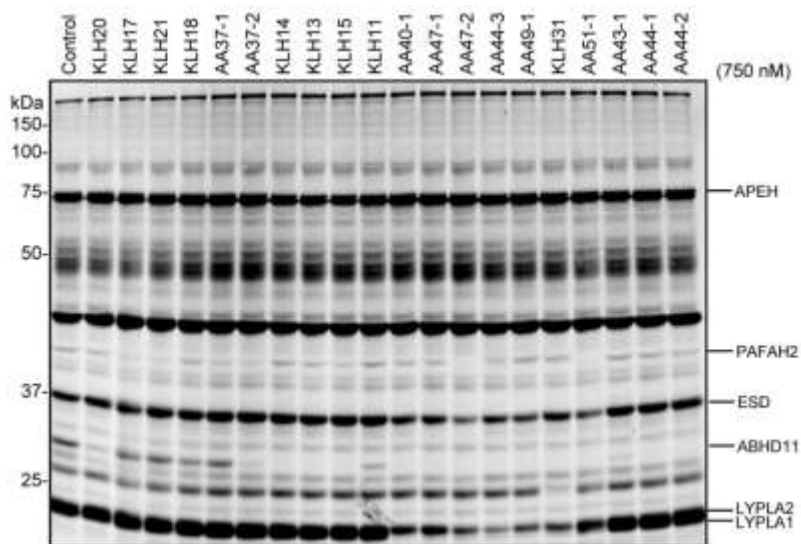
**C. 30 nM**



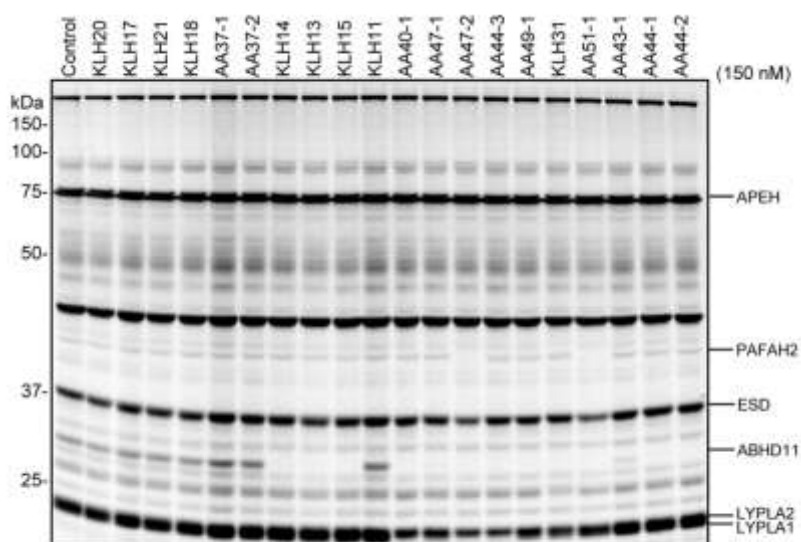
Gel-based competitive ABPP assay conducted as described in AID 493111. Control = DMSO only (no compound). See SAR **Table 4** for corresponding Entry/SID numbers. Observed anti-targets esterase D/formylglutathione hydrolase (ESD), N-acylaminoacyl-peptide hydrolase (APEH), and lysophospholipases 1 and 2 (LYPLA1 and LYPLA2). No other FP-sensitive SH anti-targets are observed out of the 20+ visible bands. Note: AA50-1 (Compound **1.16**) appears to activate several enzymes at high (1.5  $\mu$ M) concentration. Fluorescent images shown in grey scale. Gel slice at bottom of each panel shows darker scan of ABHD11 region.

**Figure 8.** Potency and selectivity of additional triazole urea synthetic library compounds at three compound concentrations: 750 nM (**A**), 150 nM (**B**), and 30 nM (**C**).

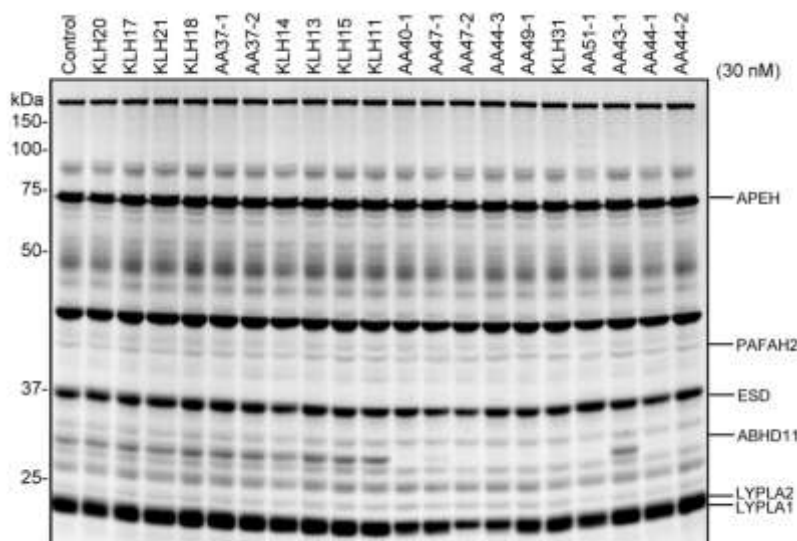
**A. 750 nM**



**B. 150 nM**



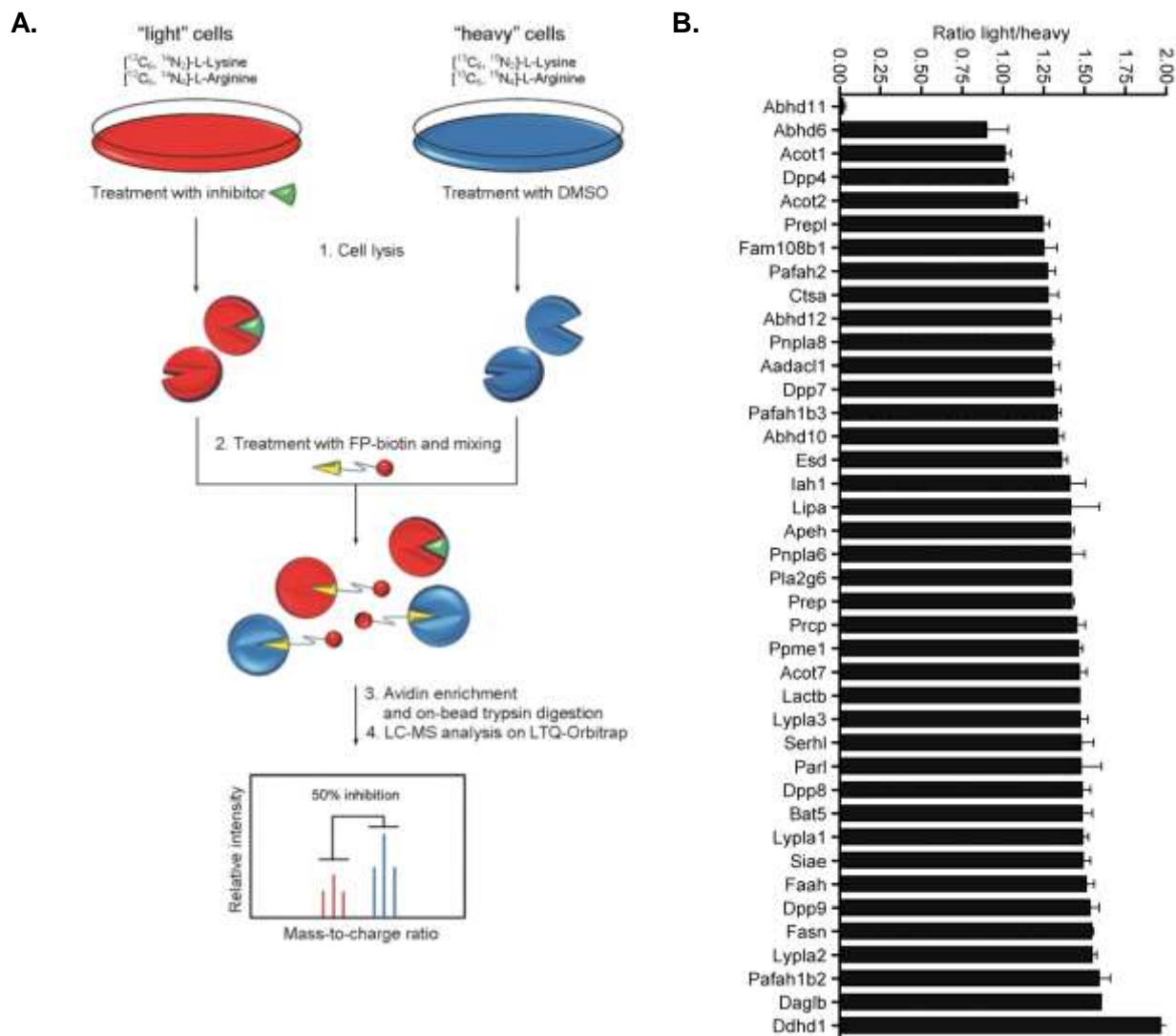
### C. 30 nM



Gel-based competitive ABPP assay conducted as described in AID 504520. Control = DMSO only (no compound). See SAR **Table 4** for corresponding Entry/SID numbers. Observed anti-targets are esterase D/formylglutathione hydrolase (ESD), platelet-activating factor acetylhydrolase type 2 (PAFAH2), lysophospholipase 1 (LYPLA1) and lysophospholipase 2 (LYPLA2). Fluorescent images shown in grey scale.

**SILAC-ABPP:** To more comprehensively identify potential anti-targets, we utilized an advanced quantitative mass spectrometry (MS)-based platform termed competitive ABPP-SILAC (**Figure 9A**). Competitive ABPP-SILAC is a merger of ABPP-MudPIT method [25] with the stable isotope labeling of amino acids in culture (SILAC) technique [26]. Competitive ABPP-SILAC allows for precise quantitation of inhibited enzymes by calculating the isotopic ratios of peptides from control- and inhibitor-treated cells. As described in AID 504522 (see also ref. [12] for similar studies with other triazole urea compounds), mouse T cells were cultured in 'light' medium (with  $^{12}\text{C}_6^{14}\text{N}_2$ -lysine and  $^{12}\text{C}_6^{14}\text{N}_4$ -arginine) or 'heavy' medium (with  $^{13}\text{C}_6^{15}\text{N}_2$ -lysine and  $^{13}\text{C}_6^{15}\text{N}_4$ -arginine). After 6 passages, near-complete (>97%) enrichment was achieved. Light and heavy cells were treated with 3 nM compound **34** (a close analog of **ML226** bearing a methoxymethyl at the 2-position of the piperidine ring instead of an ethyl), and DMSO, respectively, for four hours and then harvested, lysed, separated into soluble and membrane fractions, and treated with the affinity-tagged SH-specific probe FP-biotin (5  $\mu\text{M}$ , 90 minutes) [24]. Light and heavy fractions were then mixed (1:1 w/w), enriched with avidin, digested on-bead with trypsin, and analyzed by MudPIT LC-MS/MS [27-28] using an LTQ-Orbitrap instrument. Light and heavy signals were quantified from parent ion peaks (MS1) and the corresponding proteins identified from product ion profiles (MS2) using the SEQUEST [29] search algorithm. The depicted bar graphs represent the average ratios of light/heavy tryptic peptides for each of the SHs identified in mouse T cells. Enzymes susceptible to inhibition upon compound treatment would be expected to have light/heavy ratios significantly less than one, while uninhibited enzymes would be expected to have a ratio close to one. The results (**Figure 9B**) demonstrate that compound **34** exhibits remarkable selectivity for ABHD11, blocking >95% of activity while not affecting any of the other 40 SHs detected in T-cells.

**Figure 9.** Potency and selectivity of **34** assessed by SILAC-ABPP. **A)** Overview of the SILAC-ABPP method. **B)** Inhibition profile of **34** shows significant inhibition of only ABHD11. See AID 504522 for more details.



## 4 Discussion

Probe **ML226** (Compound **12**) was identified as a highly potent and selective covalent dual inhibitor of the target enzyme ABHD11 during the course of an inhibitor development campaign for LYPLA enzymes. The reported probe has an IC<sub>50</sub> of 15 nM and 100-fold selectivity against all other SH anti-targets surveyed by gel-based competitive ABPP (**section 3.6**). A close analog (compound **34**, SID 103913583) was shown to selectively inhibit ABHD11 *in situ* among more than 40 SHs assayed by SILAC-ABPP (**section 3.6**). **ML226** is active *in situ* (**section 3.5**), completely inhibiting ABHD11 in serum-containing media after four hours at 30 nM

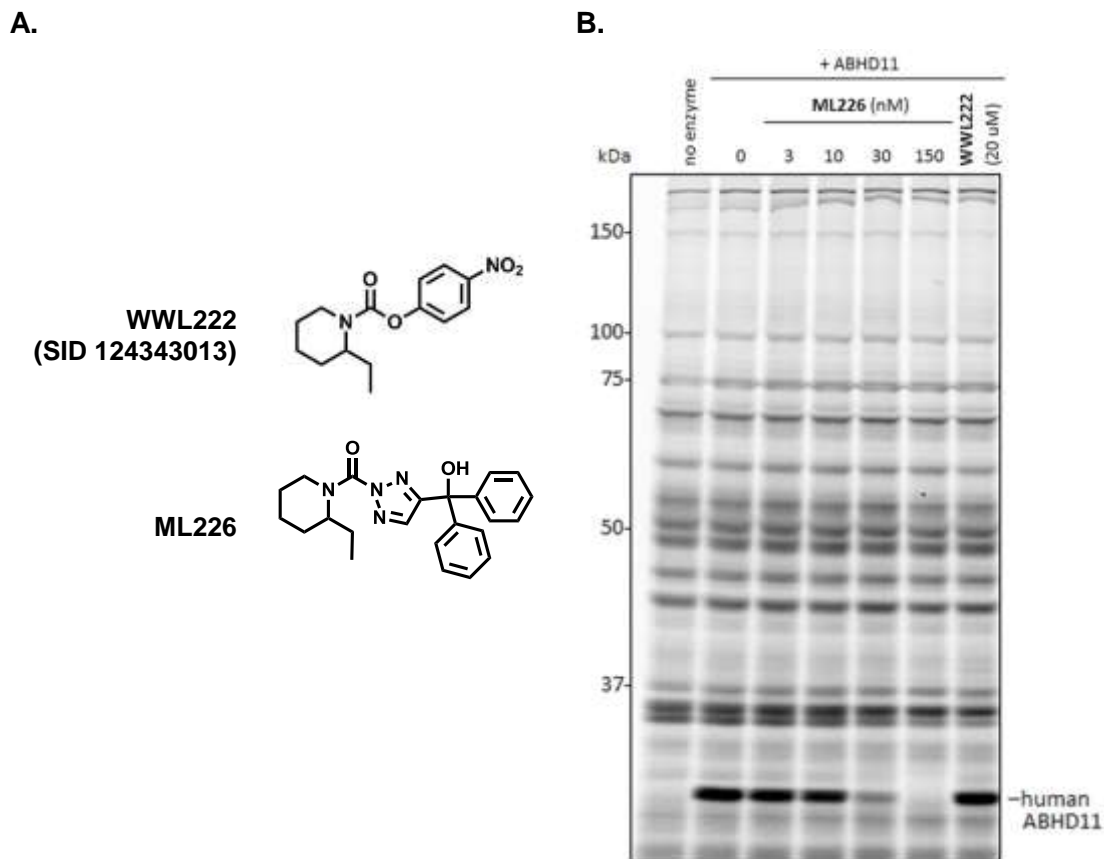
concentration. Further analysis revealed an IC<sub>50</sub> of 0.68 nM for *in situ* inhibition. **ML226** exhibits a good chemical profile: the compound is soluble in PBS at up to 27 μM, well above its active *in situ* concentration, shows no evidence of cytotoxicity up to 50 μM, and is stable in PBS for more than 48 hours. Taken together, these findings suggest that it is very possible to develop potent and selective probes based on tempered electrophilic scaffolds, and that **ML226** will be a highly successful probe for investigation of ABHD11 biology and key anti-probe for biochemical investigation of LYPLA1 and LYPLA2.

#### 4.1 Comparison to existing art and how the new probe is an improvement

As part of a super-family wide campaign to discover inhibitors for SHs, we recently reported [14] a carbamate-based inhibitor of ABHD11, **WWL222 (Figure 10A)**. Interestingly, both **WWL222** and **ML226** have a 2-ethyl substituted piperidine ring on the left hand side but different reactive elements (carbamate vs. triazole urea) and leaving groups (*p*-nitrophenyl vs. diphenylmethyl triazole). **WWL222** has an IC<sub>50</sub> of 170 nM against the mouse isoform of ABHD11, and comparable selectivity among other SHs as assessed by gel-based and LC-MS-based competitive ABPP. **WWL222** is also active *in vivo*, effecting inhibition of ABHD11 in the brains of mice upon 10 mg/kg treatment for four hours [14]. However, **WWL222** is inactive against the human isoform of ABHD11 up to 20 μM compound concentration, whereas **ML226** shows significant potency, with an IC<sub>50</sub> of less than 30 nM (**Figure 10B**). Additionally, we have yet to explore the physical (stability, solubility, reactivity) and cytotoxic properties of **WWL222**, and it is not known whether the *p*-nitrophenyl moiety will be a liability either for compound stability or as the *p*-nitrophenol metabolite released upon covalent modification. **ML226** represents an 11-fold improvement in potency relative to **WWL222** and has established desired physical attributes, including stability (>48 hours), solubility (27 μM), reactivity (none vs. 100 μM glutathione), and cytotoxicity (CC<sub>50</sub> >50 μM). Given that **ML226** is based on a different scaffold (triazole urea vs. carbamate), the two probes can also serve as mutual controls for phenotypes arising from unanticipated anti-target reactivity.



**Figure 10.** Structures (A) and competitive ABPP inhibition profiles (B) of ABHD11 inhibitors **WWL222** (SID 124343013) and **ML226**.



Gel-based competitive ABPP assay (B) conducted as described in AID 504892 with recombinant human ABHD11 spiked into mouse brain membrane proteome. For **ML226**, 75% and 100% inhibition of human ABHD11 is observed at 30 nM and 150 nM compound concentration, respectively, whereas no inhibition of human ABHD11 is observed upon treatment with 20  $\mu$ M **WWL222**. No enzyme = mouse brain membrane proteome alone with FP-Rh labeling; Control = 0 compound (DMSO only). Fluorescent image shown in grey scale.

#### 4.2 Mechanism of Action Studies

As determined from LC-MS/MS analysis (AID 504498), the probe is an activity-based inhibitor that covalently labels the active site serine nucleophile, Ser141, of ABHD11 (section 3.3). The observed mass shift of the active site peptide suggests that reaction occurs via serine nucleophilic attack on the carbonyl followed by loss of the triazole to carbamoylate the enzyme (Figure 4).

### 4.3 Planned Future Studies

Given the success of the triazole urea library, we plan to expand the library for identification of additional probes for ABHD11 (focusing on variation at the 2-position of the piperidine ring in combination with other  $R_3$  substituents) and other SHs. Additionally, we plan to more comprehensively establish parameters for *in situ* and *in vivo* use and explore the target specificity of **ML226** and compound **34** (SID 103913583) via application of alkyne analogs. For biological application, we plan to use **ML226** as a probe for investigation of the potential role of ABHD11 in Williams- Beuren syndrome, and as an anti-probe to investigate the link between LYPLA1, LYPLA2, palmitoylation, and cancer progression by 1) global proteomic and metabolomic profiling of cultured cancer cells treated with and without probe/anti-probe to identify potential metabolic pathway involvement, 2) global profiling of palmitoylation events differentially regulated in cancer cells treated with and without probe/anti-probe, and 3) evaluating the role of LYPLA1 and LYPLA2 in cancer pathogenesis using assays that measure proliferation, migration, and invasion *in situ*. Future studies may also extend to the nervous system, where LYPLA1 has been implicated in regulating dendritic spine morphogenesis, presumably through regulating dynamic palmitoylation of key dendritic signaling and scaffolding proteins [30].

## 5 References

1. Martin, B.R. and B.F. Cravatt, *Large-scale profiling of protein palmitoylation in mammalian cells*. Nat. Methods, 2009. **6**(2): p. 135-8.
2. Dekker, F.J., et al., *Small-molecule inhibition of APT1 affects Ras localization and signaling*. Nat. Chem. Biol., 2010. **6**(6): p. 449-56.
3. Bachovchin, D.A., et al., *Identification of selective inhibitors of uncharacterized enzymes by high-throughput screening with fluorescent activity-based probes*. Nat. Biotechnol., 2009. **27**(4): p. 387-94.
4. Schubert, C., *The genomic basis of the Williams-Beuren syndrome*. Cell. Mol. Life Sci., 2009. **66**(7): p. 1178-97.
5. Duncan, J.A. and A.G. Gilman, *A cytoplasmic acyl-protein thioesterase that removes palmitate from G protein alpha subunits and p21(RAS)*. J. Biol. Chem., 1998. **273**(25): p. 15830-7.
6. Sugimoto, H., H. Hayashi, and S. Yamashita, *Purification, cDNA cloning, and regulation of lysophospholipase from rat liver*. J. Biol. Chem., 1996. **271**(13): p. 7705-11.
7. Toyoda, T., H. Sugimoto, and S. Yamashita, *Sequence, expression in Escherichia coli, and characterization of lysophospholipase II*. Biochim. Biophys. Acta, 1999. **1437**(2): p. 182-93.
8. Biel, M., et al., *Synthesis and evaluation of acyl protein thioesterase 1 (APT1) inhibitors*. Chemistry, 2006. **12**(15): p. 4121-43.
9. Deck, P., et al., *Development and biological evaluation of acyl protein thioesterase 1 (APT1) inhibitors*. Angew. Chem. Int. Ed. Engl., 2005. **44**(31): p. 4975-80.
10. Jessani, N., et al., *Enzyme activity profiles of the secreted and membrane proteome that depict cancer cell invasiveness*. Proc. Natl. Acad. Sci. U. S. A., 2002. **99**(16): p. 10335-40.
11. Leung, D., et al., *Discovering potent and selective reversible inhibitors of enzymes in complex proteomes*. Nat. Biotechnol., 2003. **21**(6): p. 687-91.

12. Adibekian, A., et al., *Click-generated triazole ureas as ultrapotent in vivo-active serine hydrolase inhibitors*. Nat. Chem. Biol., 2011. **7**(7): p. 469-78.
13. Forner, F., et al., *Quantitative proteomic comparison of rat mitochondria from muscle, heart, and liver*. Mol. Cell. Proteomics, 2006. **5**(4): p. 608-19.
14. Bachovchin, D.A., et al., *Superfamily-wide portrait of serine hydrolase inhibition achieved by library-versus-library screening*. Proc. Natl. Acad. Sci. U. S. A., 2010. **107**(49): p. 20941-6.
15. Li, X., et al., *Characterization of dasatinib and its structural analogs as CYP3A4 mechanism-based inactivators and the proposed bioactivation pathways*. Drug Metab. Dispos., 2009. **37**(6): p. 1242-50.
16. Li, X., T.M. Kamenecka, and M.D. Cameron, *Bioactivation of the epidermal growth factor receptor inhibitor gefitinib: implications for pulmonary and hepatic toxicities*. Chem. Res. Toxicol., 2009. **22**(10): p. 1736-42.
17. Kalisiak, J., K.B. Sharpless, and V.V. Fokin, *Efficient synthesis of 2-substituted-1,2,3-triazoles*. Org. Lett., 2008. **10**(15): p. 3171-4.
18. Moore, S.A., et al., *Identification of a high-affinity binding site involved in the transport of endocannabinoids*. Proc. Natl. Acad. Sci. U. S. A., 2005. **102**(49): p. 17852-7.
19. Alexander, J.P. and B.F. Cravatt, *The putative endocannabinoid transport blocker LY2183240 is a potent inhibitor of FAAH and several other brain serine hydrolases*. J. Am. Chem. Soc., 2006. **128**(30): p. 9699-704.
20. Lowe, D.B., et al., *In vitro SAR of (5-(2H)-isoxazolonyl) ureas, potent inhibitors of hormone-sensitive lipase*. Bioorg. Med. Chem. Lett., 2004. **14**(12): p. 3155-9.
21. Ebdrup, S., et al., *Synthesis and structure-activity relationship for a novel class of potent and selective carbamoyl-triazole based inhibitors of hormone sensitive lipase*. J. Med. Chem., 2004. **47**(2): p. 400-10.
22. Johnson, D.S., E. Weerapana, and B.F. Cravatt, *Strategies for discovering and derisking covalent, irreversible enzyme inhibitors*. Future Med. Chem., 2010. **2**(6): p. 949-964.
23. Vincent, P.W., et al., *Anticancer efficacy of the irreversible EGFr tyrosine kinase inhibitor PD 0169414 against human tumor xenografts*. Cancer Chemother. Pharmacol., 2000. **45**(3): p. 231-8.
24. Robertson, J.G., *Mechanistic basis of enzyme-targeted drugs*. Biochemistry, 2005. **44**(15): p. 5561-71.
25. Jessani, N., et al., *A streamlined platform for high-content functional proteomics of primary human specimens*. Nat. Methods, 2005. **2**(9): p. 691-7.
26. Mann, M., *Functional and quantitative proteomics using SILAC*. Nat. Rev. Mol. Cell Biol., 2006. **7**(12): p. 952-8.
27. Wolters, D.A., M.P. Washburn, and J.R. Yates, 3rd, *An automated multidimensional protein identification technology for shotgun proteomics*. Anal. Chem., 2001. **73**(23): p. 5683-90.
28. Washburn, M.P., D. Wolters, and J.R. Yates, 3rd, *Large-scale analysis of the yeast proteome by multidimensional protein identification technology*. Nat. Biotechnol., 2001. **19**(3): p. 242-7.
29. MacCoss, M.J., C.C. Wu, and J.R. Yates, 3rd, *Probability-based validation of protein identifications using a modified SEQUEST algorithm*. Anal. Chem., 2002. **74**(21): p. 5593-9.
30. Siegel, G., et al., *A functional screen implicates microRNA-138-dependent regulation of the depalmitoylation enzyme APT1 in dendritic spine morphogenesis*. Nat. Cell Biol., 2009. **11**(6): p. 705-16.